MDPI

Review

Progress in Achieving Fire-Retarding Cellulose-Derived Nano/Micromaterial-Based Thin Films/Coatings and Aerogels: A Review

Irina Turku *, **Anti Rohumaa** [ID], **Tapio Tirri and Lasse Pulkkinen**

FiberLaboratory, South-Eastern Finland University of Applied Science, Vipusenkatu 10, 57200 Savonlinna, Finland; anti.rohumaa@xamk.fi (A.R.); tapio.tirri@xamk.fi (T.T.); lasse.pulkkinen@xamk.fi (L.P.)
* Correspondence: irina.turku@xamk.fi; Tel.: +358-505995888

Abstract: The enormous potential of renewable bioresources is expected to play a key role in the development of the EU's sustainable circular economy. In this context, inexhaustible, biodegradable, non-toxic, and carbon-neutral forest-origin resources are very attractive for the development of novel sustainable products. The main structural component of wood is cellulose, which, in turn, is the feedstock of nanocellulose, one of the most explored nanomaterials. Different applications of nanocellulose have been proposed, including packaging, functional coatings, insulating materials, nanocomposites and nanohybrids manufacturing, among others. However, the intrinsic flammability of nanocellulose restricts its use in some areas where fire risk is a concern. This paper overviews the most recent studies of the fire resistance of nanocellulose-based materials, focusing on thin films, coatings, and aerogels. Along with effectiveness, increased attention to sustainable approaches is considered in developing novel fire-resistant coatings. The great potential of bio-based fire-resistant materials, combined with conventional non-halogenated fire retardants (FRs), has been established. The formulation methods, types of FRs and their action modes, and methods used for analysing fireproof are discussed in the frame of this overview.

Keywords: nanocellulose; coatings; fire retardancy; phosphorylation; nanomaterials; aerogels

1. Introduction

Developing a "green" circular economy is highly dependent on the quality and availability of raw sustainable materials. In this regard, lignocellulose (LC), the most abundant renewable biomass in the biosphere with a global annual production of 181.5 billion tons [1], is of great interest as a natural raw material for producing value-added products. Lignocellulosic material is typically derived from agro-waste, forest trees, and grasses. LCs consist mainly of the polymers that form plant cell walls, celluloses (40–45 wt%), hemicelluloses (15–35 wt%), and lignin (20–40 wt%) [1]. Two approaches to LC biomass conversion into value-added products are used: lignocellulosic biorefining and syngas production [1]. Syngas produced by LC biomass gasification can be used as feedstock for fuel and chemical manufacturing. In lignocellulosic biorefining, the biomass is separated into its constituents, cellulose, hemicelluloses, and lignin, followed by their conversion into bio-based chemicals and materials. The cellulose-derived nanomaterials, nanocrystalline and nanofibrillated cellulose, are of particular interest. Nanocelluloses combining unique properties, such as outstanding mechanical stability, low density, large specific surface area, high aspect ratio, and biocompatibility, are a material of increasing interest in packaging and protective coating fields, the implant industry, separation technology, adhesives, and many others [2,3]. Significant progress in cellulose-based nanocomposites, including aerogels, has been reported [4].

Depending on the technique used, cellulose pulp can be processed into nanocrystalline cellulose (NCC) and nanofibrillated cellulose (NFC). NCCs, rod-like particles 3–5 nm in

diameter and 50–500 nm in length [5], are obtained via hydrolysis of the amorphous region of the cellulose backbone using a mineral acid, typically sulfuric acid [3,6,7]. Partial chain hydrolysis yields microcrystalline cellulose (MCC), with a particle diameter of 10–50 μm [5] and degree polymerization (DP) between 150 and 300 [8]. NFCs, typically 4–20 nm in diameter and 0.5–2 μm in length [5], are produced through the mechanical treatment of the cellulose fibres. However, NFC slurry can contain micro-sized fibres, referred to as microfibrillated cellulose (MFC), the particle size of which ranges between 10–100 nm in diameter and 0.5–10's μm in length [5]. The mechanical treatment can be performed using a grinder, microfluidizer, high-pressure homogeniser, twin-screw extruder (TSE), or high-speed blender [9–14].

Because the fibrils are combined and kept together by extensive hydrogen bonding, significant energy input is required to disintegrate them. In this respect, an enzymatic or chemical pre-treatment is used to easily dismantle the fibrils. The functionalisation of cellulose fibres by charged moieties facilitates the delamination process due to the swelling of the fibres from increased osmotic pressure inside the fibre wall and electrostatic repulsion [10]. TEMPO (2,2,6,6-Tetramethylpiperidine 1-oxyl) oxidation is the most common method used to pre-treat cellulose fibres [15]. Other methods have also been reported, such as etherification [16], periodate oxidation [9], enzymatic hydrolysis [17], and phosphorylation [10,18,19]. Notably, the crystalline structure of cellulose is retained after mechanical treatment even when combined with chemical modification [14].

The combination of outstanding mechanical performance (tensile modulus at about 143 GPa) [20], biocompatibility, high surface area, transparency, and reactivity makes NC suitable for use as a reinforcing material and as a substrate for the production of thin films, coatings, and aerogels. The basic approaches to fabricating NC-derived films and nanopapers are casting, coating, papermaking, and extrusion [2]. Recently, a novel layer-by-layer (lbl) deposition for coating processing has been applied. The lbl assembly process predominantly relies on electrostatic interactions between polyelectrolytes and charged nanoparticles [21]. Bio-based aerogels are commonly formed by a novel freeze-drying procedure, also known as lyophilisation [4]. Unlike the supercritical drying process used for aerogels made from silica and other conventional materials, freeze-drying results in a highly aligned, honeycomb-like pore structure, yielding higher mechanical performance than conventional foams [22].

One of the critical limitations of cellulose is its intrinsic flammability, which restricts the exploitation of cellulose-based materials. Fire protection technology offers various treatments and fire retardants to minimise the fire risk of materials and products. Efficiency, applicability, and cost are parameters normally considered in fire retardant selection, but increasingly demanding ecological requirements [23] have encouraged researchers and manufacturers to design sustainable FR systems without a toxic footprint.

Three factors are required for combustible material burning: fuel, heat, and oxygen, which form the well-known "fire triangle" [24]. At least one of these components must be removed to suppress the fire. When FRs are incorporated, the combustion process becomes controlled in condensed or vapour phases through FR action by chemical or physical means. Based on their chemistry, FRs are divided into phosphorous- and nitrogen-containing, halogenated, metal hydroxides and oxides, borates, and nanometric particles [24].

Inorganic metal hydroxides, particularly $Al(OH)_3$, are the most used FR, followed by halogen-containing [25]. Metal hydroxides physically dilute combustible matter, as well as release water vapor at high temperatures, which dilutes the flaming gases and sinks the heat [24,26]. To achieve a significant effect, up to 60% by weight of metal hydroxides is required, which can negatively influence the mechanical performance of the material. Halogen-containing FRs work in the vapour phase, scavenging reactive radicals, $H^{\bullet}$, and $OH^{\bullet}$, thereby inhibiting flame. They are recognised as effective, but their use is prohibited due to their high toxicity, low degradability, and tendency to accumulate in the biotic and abiotic systems of the environment [23]. The phosphorus-based FRs (P-FRs) are the third most used FRs, and the number of applications for them is growing. The advantage of

P-FRs is that they work in both condensed and gas phases. Thus, similarly, to halogenated FRs, P-FRs trap reactive radicals, and their effectiveness is five times higher than that of bromide and ten times higher than chlorine [24,27]. In the condensed phase, P-FRs act through the barrier effect, facilitating char synthesis, particularly in oxygen-containing polymers, such as cellulose, polyester, and polyamides [24,27]. Nitrogen-based FRs, which can be ammonia- or melamine-based, endothermically vaporise to ammonia or N_2 to dilute heat and flammable gases. N- and P-based FRs are often combined due to their synergistic effect [27]. Here, nitrogen catalyses the phosphorylation of cellulose, facilitating crosslinking of FR within the polymer network, which promotes char formation [28]. Yet, N- and P-containing FRs are common components in the intumescent FR system, a special case of fireproofing. Three components make up the intumescent formulation, (i) dehydrating agent or acid source (e.g., phosphoric acid and ammonium polyphosphate APP), which reacts with (ii) char-forming ingredients (e.g., polyols, cellulose), and (iii) a blowing agent (e.g., melamine) that generates inert gas, which, in turn, expands the char [29]. Intumescent coatings swell when a critical temperature is reached, typically around 200 °C, to form a dense charred layer, which is an effective barrier against the transfer of combustible gases as well as a shield for the substrate against heat and flame [24]. An intumescent system based on expandable graphite (EG) works in the same way [30,31]. EG is a partly oxidised form of graphite, where an oxidising agent, commonly sulfuric acid, is intercalated between the graphite layers. Upon heating, the acid evaporates, causing irreversible expansion of the graphite, up to 300 times its initial volume [30].

Boron-based chemicals, boric acid, and its salts are widely used commercial flame retardants for wood and wooden products. At elevated temperatures, they decompose endothermically, evolving water and forming a glassy melt on the surface of the substrate. In addition, boric acid esterifies the OH groups of cellulose, promoting carbonaceous char formation [32]. However, due to ecological issues, boric acid is a candidate for the registration, evaluation, authorisation and restriction of chemicals (REACH) list, being a substance of very high concern (SVHC) due to its negative impact on the reproductive system [23].

Nanotechnology is one of the fastest-growing fields in science and materials engineering. Nanotechnology represents a great opportunity for designing novel materials with better mechanical, physical, and barrier performance, including fire resistance. The nanoclays (e.g., montmorillonite (MMT) and sepiolite (Sep)) are most frequently used nanoadditives to improve the thermal stability of polymers [33,34] and wooden materials [35–38]. Other nanofillers, such as carbon-based, carbon nanotubes (CNT) [39,40], EG [30,31,41], and graphene [42,43], the metal oxides, TiO_2, ZnO [40,44–47], SiO_2 [45,48], MoS_2 [49], and recently explored MXene [50–52] and metal-organic frameworks (MOFs) [53–56], also show potential as FR additives in coatings, aerogels, polymer, and wooden materials.

During the search for novel "green" fire safety materials, significant attention has been paid to bio-inspired FR additives, such as desoxyribonucleic acid (DNA) [57], proteins [58], starch [59], chitosan [60,61], lignin [62], and phytic acid [63]. The fire retardancy mechanism of these additives is commonly related to char-forming ability. Thus, the aromatic structure of lignin ensures the formation of stable carbonised residue during combustion, especially the phosphorylated form of lignin [62]. Starch and chitosan are natural polyols that form a carbonaceous layer when burned [59,61]. In addition, amino polysaccharide chitosan releases ammonia, causing the exfoliation of the residue [61]. Proteins containing sulfur and nitrogen (e.g., hydrophobins) and phosphate groups (e.g., casein) catalyse charring during cellulose burning [57,60]. In a DNA molecule, the presence of phosphoric acid (acts as acid catalyst), a nitrogen-containing moiety which releases ammonia (acts as a blowing agent), and deoxyribose (char source) make it an intrinsically intumescent FR compound [57]. Plant seed-derived phytic acid (PA) is a natural catalyst of charring due to its high phosphorus content, 28 wt%, from phosphoric acid residues [63].

The growing interest in applications of nano/microcellulose and recent achievements in nanocellulose materials manufacturing also facilitate research interest in cellulosic ma-

terial modification in terms of reaching the desired functionality. The present work aims to summarise the main methods for improving the fire resistance of thin films, coatings, and aerogels prepared from cellulose sub-sized derivates, MFC, NFC, MCC, and NCC, by reviewing the research published during the last decade. The first part discusses different approaches towards phosphorylating cellulosic materials to induce intrinsic fireproofing. The following sections outline the application of nanosized additives alone or in combination with non-halogenated conventional and biobased FRs. The modes of action of FRs and the techniques used for thermal properties and fire retardancy analysis are also reported.

2. Methods of Nanocellulose Phosphorylation and Their Effects on FR Properties

Charring is a crucial mechanism for the fire retardancy of synthetic and natural polymers. Generally, char is formed at the expense of flammable gases and acts as a physical barrier that lowers the transfer of flame-supporting sources in and out of the burning underlayer. Due to its chemical structure $(C_6H_{10}O_5)_n$, cellulose can produce carbonaceous residue (char) 44.4% of the initial mass [64]. However, cellulose combustion at favourable conditions, e.g., dry, hot, and energetic environments, generates levoglucosan, which in turn readily decomposes to flammable gases. In practice, the maximum char yield is 12–15%, depending on the peak temperature reached [64]. Another route is the dehydration and decomposition of glycosidic units to form aromatic char, Figure 1.

One way to enhance the intrinsic fire retardancy of cellulose is by directly incorporating phosphorus-containing components into the cellulose structure. The cellulose molecule is abundant in hydroxyl groups, which makes it highly reactive and easy to functionalize. Each glycosidic unit of cellulose has three OH groups at C2, C3, and C6. Comparing their reactivity, the OH group at C6 is ten times more reactive than the other two [65], so it has an important role in cellulose modification, including phosphorylation. In this scenario, the undesired levoglucosan that forms due to C1 and C6 intramolecular cyclisation can be inhibited by blocking the C6 hydroxyl by the formation of a phosphorus ester, thereby redirecting the burning route to char formation, Figure 1.
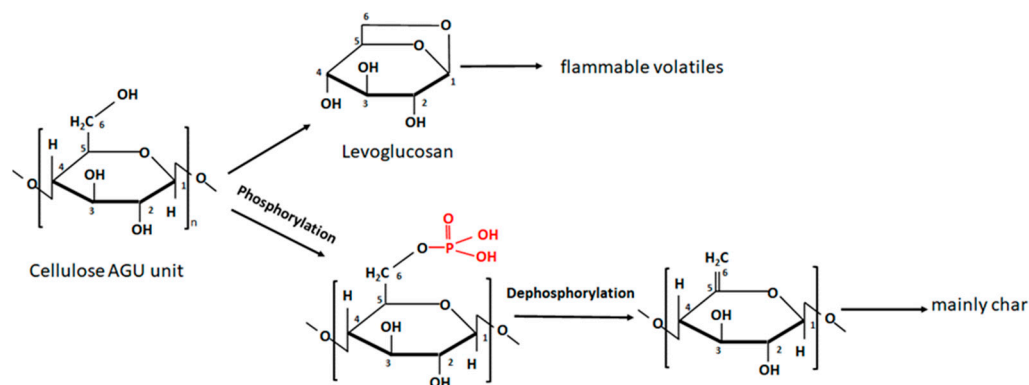

Figure 1. Two competing reaction routes for cellulose thermal oxidation: (top) levoglucosan formation at favourable conditions; (bottom) C6 phosphorylation-dephosphorylation routes (Adapted from [66,67]).

Furthermore, phosphoric acid, initially released at elevated temperatures, catalyses the dehydration of cellulose and char formation [10]. The phosphorylation reactions of cellulose can be triggered by phosphorus acid, H_3PO_3 [68,69], orthophosphoric acid, H_3PO_4 [70,71], or their salts [10,14,18,72], phosphorus pentoxide P_5O_{10} [73–75], periodate oxidation [9], phytic acid [76,77], enzymes [78], and through the grafting of phosphorus-containing polymers [60,70]. Cellulose-rich fibres are typically phosphorylated in presence of urea or less commonly used solvents such as N,N-dimethylformamide (DMF) and pyridine [10,60,70,76]. Urea prevents the degradation of the cellulose during curing, assists in the disruption of the hydrogen bonds between the cellulose nanocrystals, preventing their aggregation, and increases the penetration of phosphate moieties into the core of the

fibres [10,18,70,73,76]. The extent of the phosphorylation or degree of substitution (DS) is defined as the average number of P atoms per cellulose monosaccharide unit [79]. The DS depends on many factors, such as the type of modifying agent, reagent-to-substrate ratio, assisting additives, and ambient conditions [10,71–73,79]. Typically, phosphorylation efficiency can be evaluated by potentiometric titration, Fourier transform infrared (FTIR) spectroscopy, and nuclear magnetic resonance (NMR) techniques [71]. The results of various methods of nanocelluloses pre- and post-phosphorylation, under different conditions and methods, are presented in Table 1.

Table 1. Selected examples of pre- and post-phosphorylation of cellulosic materials.

Cellulose Grade	Reagent	Charge/DS, μeq/μmol g^{-1}, (0–1)	UL-94	TGA/Air Residue, wt%	TGA/Air T_{max2}, °C	Source
NFC	Control/unmodified	-	-	~0 (800 °C)	422	[10]
	AGU/(NH$_4$)$_2$HPO$_4$/urea = 1/1.2/4.9 [a]	912/0.15	self-exting. [c]	9	539	
NFC (post-P)	Control/unmodified	-	-	15 (600 °C)	-	[78]
	Hexokinase (EC2.7.1.1.)/ATP/MgCl$_2$	DS: 0.43	-	57	-	
NFC	Control/unmodified	-	-	0	-	[19]
	AGU/(NH$_4$)$_2$HPO$_4$/urea = 1/1.2/4.9 [a]	2930	V-0	~25 (800 °C)		
NFC	Control	-	-	0.6 (800 °C)	-	[75]
	P$_2$O$_5$/cellulose = 1:1 and 2:1 [b]; (+melamine)	DS: 0.15–0.16	-	9.2	-	
NCC (post-P)	Control/unmodified	-	-	3 (500 °C)		[73]
	P$_2$O$_5$/urea	3300/0.26	-	30		
	P$_2$O$_5$	950/0.08				
NFC/MFC	AGU/(NH$_4$)$_2$HPO$_4$/urea = 1/1.5/10 [a]	1900/0.39	self-exting. [c]	-	-	[11]
NFC	Control/unmodofoed	0	-	0 (700 °C)	379	[9]
	Periodate oxidation	320	self-exting. [c]	27	389	
NFC/MFC	Control/unmodified	-	-	0.6 (800 °C)	513	[80]
	AGU/(NH4)2HPO4/urea = 1/0.5/2 [a]	1540	self-exting. [c]	20	625	
NCC/NFC (post-P)	Control/unmodified	-	-	~14 (600 °C)	-	[71]
	NC/H$_3$PO$_4$/water	NFC: 19		~30	-	
		NCC: 435	-	~45	-	
			-			
	NC/H$_3$PO$_4$/molten urea	NFC: 1173	-	~45	-	
		NCC: 1038	-	~40	-	

[a] molar ratio; [b] mass ratio; [c] standard does not define.

The use of phosphorous-based media for facilitating nanofibrillation of cellulose and inducing fireproofing properties to the end product was first proposed by Ghanadpour et al. [10]. In this research, the pulp cellulose was pre-treated with a (NH$_4$)$_2$HPO$_4$/urea mixture, with the molar ratio of AGU/(NH$_4$)$_2$HPO$_4$/urea equal to 1/1.2/4.9. The modified pulp was dried at 70 °C and cured at a temperature of 150 °C (10–90 min); the fibres were then disintegrated using a high-pressure microfluidizer. The maximal total charge of 912 μeq g^{-1} was achieved after a 1 h curing period, then declined after extended curing time due to fibres delamination. P-NFC-based film prepared by membrane filtration showed a self-extinguishing property leaving 92 wt% of residue in the flame test and increased mass residue in TGA. Notably, the thermal stability of the formed char was increased which indicated the second T_{max2} value, Table 1. More recently, Hou et al. used a similar phosphorylation protocol, high-speed blender and membrane filtration technique to prepare a nano/microfibrillated cellulose-based film with significant fireproof, transparency, and mechanical performance [11]. Authors proposed that synthesised high-quality film could replace synthetic plastic in demanding applications, such as light management layers of photoelectronic devices. The lbl self-assembly technique was utilized in creating an ultrastrong and flame-resistant film by combining phosphorylated (anionic) and aminated (cationic) NFC in reference [81]. The fireproofing of the film was achieved through close contact and strong interaction between layers induced by lbl structuring as well as N-P synergistic FR effect. Moreover, the composite material's tightly packed structure played a significant role in its exceptional mechanical properties. Sirviö et al. used periodate oxidation to produce thermally stable NFC grade [9]. Thermo-oxidative TGA measure-

ments showed that modified NFC left up to 27 wt% thermally stable residue whereas non-modified NFC almost completely burned.

　　Reducing processing costs is crucial for scaling the production and application of nanocellulose-based products. In conventional processes, nanofibrillated products have a low consistency, typically 2 wt%, and are characterised by high energy consumption, making these processes unsustainable. In this context, Rol and co-workers have proposed the nanofibrillation of chemically (TEMPO-oxidised) or enzymatically treated cellulose using twin-screw extrusion (TSE), which allowed processing at high solid contents, 20–25 wt%, while reducing the energy input by 60% compared to the conventional technique [82]. Later, Rol et al. used pre-phosphorylated pulp cellulose and energy-effective TSE for processing FR NFC grade [19]. The phosphorylation was performed following the protocol of Ghanadpour et al. [10], resulting in phosphate loading up to 2930 µmol g^{-1} (Table 1). Notably, the phosphorylation degree did not change after the nanofibrillation step. The nanopaper from P-NFC achieved the class of V-0 in the UL-94 test [83].

　　The synergistic effect of phosphorus-based FR and lignin on the fire retardancy of NFC film has been demonstrated by Zhang et al. [14]. In this research, bamboo pulp cellulose, with or without lignin, was pre-phosphorylated with $(NH_4)_2HPO_3$/urea. Next, the cellulosic fibres were exfoliated to nanofibrils in a Masuko Sangyo MKCA6-2 grinder. The flame retardancy of the films produced by the solvent casting method was studied with microscale combustion calorimetry (MCC), and the results are shown in Table 2. Phosphorylation or the presence of lignin facilitated the fireproofing of the cellulose; however, samples prepared from lignin-containing phosphorylated pulp had the best performance. The high fire retardancy was due to double protection: (i) a P_xO_y-composed layer originating from the P-moiety of grafted NFC, (ii) the diluting effect of non-combustible gases (H_2O, CO, CO_2) release, and (iii) a barrier carbon layer due to carbonation of P-NFC with further enrichment through lignin involvement.

Table 2. Micro-scale combustion calorimetry test results. BNFC denotes bamboo NFC, P denotes phosphorylation, and L denotes lignin [14].

Sample	HRC, J g^{-1} K^{-1}	pHRR, W g^{-1}	T$_{pHRR}$, °C	THR, kJ g^{-1}
BNFC	168.9	166.2	356.1	9.7
P-BNFC	43.2	42.7	293	1.8
BNFC-L	135.6	134.2	339.3	8.3
P-BNFC-L	22.8	21.1	281.2	1.3

HRC—heat release combustion; pHRR—peak of heat release rate; THR—total heat release.

　　Wu et al. used a mechanochemical approach to process the phosphorylated grade of NFC from corn cellulose [75]. The cellulose powder was ball-milled in an agitate jar in the presence of phosphorus pentoxide, P_4O_{10}, achieving a DS of 0.16 (Table 1). The fire retardancy was additionally stimulated by modifying the P-NFC with melamine. The melamine and P-NFC were combined through ionic bonding, which was confirmed by FTIR spectroscopic analysis. Incorporating 30 wt% of fire-retarded NFC into the bamboo paper induced self-extinguishing properties, and the limiting oxygen index (LOI) increased to 30%. Besides, the calorimeter test showed that the (pHRR) of the modified paper decreased by ca. 63% and the (THR) by more than 70% compared to the control. In another work, Fiss et al. used a ball milling method for NCC post-phosphorylation with P_4O_{10} crystals [73]. In this case, the phosphorylation was performed with and without the assistance of additives, such as urea, tetramethylurea, 2-imidazolidone, or salt urea phosphate. The best result was obtained in the presence of urea, where the phosphate amount reached 3300 µmol g^{-1}, whereas, without urea, the phosphorylation value was only 950 µmol g^{-1}. Notably, mechanochemical phosphorylation resulted in higher phosphorylation than that reported by Kokol et al., 1038 µmol g^{-1}, who used liquid-phase phosphorylation [71]. However, the TGA showed that NCC liquid-phase phosphorylation (in molten urea) resulted in lower mass loss, ca. 60 wt%, than the sample in solid-state conditions, which had a mass loss of

70 wt%, obtained by Fiss et al. [73]. The positive role of urea has been demonstrated by Kokol et al., who compared the phosphorylation of the nanocelluloses NCC and NFC in heterogeneous (H_3PO_4/water) and homogeneous (H_3PO_4/molten urea) conditions [71]. According to the results obtained, the charge density for samples modified in a homogeneous environment was significantly higher than those modified in the H_3PO_4/water solution (Table 1).

More recently, Khakalo et al. have proposed an effective fibrillation method for fireproof MFC production in which enzymatically aided pulp fibres, denoted as high consistency enzymatically fibrillated cellulose (HefCel), are impregnated with a phosphorylation agent, $(NH_4)_2HPO_4$/urea [80]. This protocol obtained a nano(micro)fibrillated (NMFC) cellulose with high solid content, 25 wt%, and low energy consumption. The thermo-oxidative TGA demonstrated that the functionalised samples were more sensitive to heating, resulting in significant early degradation due to phosphoric acid release; however, there was significant increased char residue, as seen in Table 3. Moreover, the remarkably increased the second T_{max2} indicated the high thermal stability of formed char. A vertical flame test showed that the burning rate of the P-HefCel film decreased with increasing degree of phosphorylation; the sample with the highest charge content, 1540 μmol g^{-1}, was self-extinguishing, leaving ca. 89% residue by weight.

Table 3. Two-step degradation of HefCel and P-HefCel samples at various AGU/$(NH_4)_2HPO_4$ molar ratios [80].

Sample	$T_{10\%}$, °C	$T_{50\%}$, °C	T_{max1}, °C	T_{max2}, °C	Char, wt%
HefCel	285.2	347.2	346.8	512.5	0.6
P-HefCel_0.125 *	226.4	330.4	268.2	529.2	2.2
P-HefCel_0.25 *	232.4	361.2	284.5	552.2	9.2
P-HefCel_0.5 *	210.6	401.4	280.4	624.8	20.0

* Number denotes an AGU/$(NH_4)_2HPO_4$ molar ratio.

The phosphorus for phosphorus-based FRs is currently obtained from phosphate rock, and due to the limited amounts available, the EU Commission included phosphate rock in its list of critical materials in 2014 and added elemental phosphorus in 2017 [84]. In this background, biobased phytic acid, typically found in beans and grains, is a sustainable alternative for P-containing mineral-derived FRs [63]. When subjected to flame, PA releases a phosphoric acid, amount of which is sufficient for catalysing crosslinking and charring of cellulose. Yuan et al. have used PA in the presence of urea/cyandiamide to functionalise MCC [77]. The pyrolysis combustion flow calorimetry (PCFC) data of neat and phosphorylated MCC with PA (30 and 50%) are shown in Table 4. The main parameters characterising fire resistance were improved with PA incorporation, and the effect of treatment with 50% PA was more significant.

Table 4. PCFC data of PA-MCC obtained at various concentrations of PA [77].

Sample	HRC, J g^{-1} K^{-1}	pHRR, W g^{-1}	THR, kJ g^{-1}	Char, wt%
MCC	351.0	343.3	12.7	1.1
MCC/30%-PA	197.0	193.5	7.6	17.5
MCC/50%-PA	68.0	64.7	2.0	33.5

Another example of a green method for cellulose phosphorylation is using adenosine-5′-triphosphate (ATP), each molecule of which contains three moieties of phosphate. Božič et al. have used enzymatic phosphorylation of NFC in the presence of Mg ions and ATP [78]. Enzyme hexokinase catalyses the transfer of the phosphoryl groups of ATP to oxygen at C6 of the cellulose units. A high DS, up to 0.43, was achieved without additional pre-treatment or/swelling steps. The TGA showed a significant increase in the mass of residue from P-NFC, which was adjusted to 57% at 600 °C (Table 1).

This section provides information about the effectiveness of phosphorylation in modifying nano/microcellulose for enhancing fire retardancy and thermal stability. The addition of phosphorus-containing groups to nanocellulose results in materials that can self-extinguish, thus making them suitable for fire-retarding coatings, even in high-demand applications like electronics. This modification also enhances the mechanical performance of the resulting films by creating extra hydrogen bonds between the cellulose fibrils [14].

The phosphorylation method can facilitate cellulose fibrillation and make it fireproof by attaching phosphate groups to the cellulose backbone. Chemically induced fire resistance is typically more stable compared to physically mixing with FR additives. Physically incorporated additives can be leached during exploitation, resulting in a decline in properties and environmental pollution. However, the main drawback of conventional phosphorylation methods is that they require a curing step at a high temperature averaging 150 °C. The high temperature can cause undesired colour changes in cellulose. Additionally, urea which is typically used as a co-agent during the phosphorylation is decomposed to ammonia upon heating. Contact with ammonia can irritate skin, eyes, nose, and throat. As an alternative, enzymatic phosphorylation can transfer phosphate-moiety from ATP to polymer without the use of urea, resulting in even higher DS and char residue parameters compared to conventional methods [78].

3. Combination of Conventional Fire Retardants with Nanosized Additives

3.1. Nanoclays Case Study

One of the most frequently utilised additives in nanocellulosic, as well as synthetic polymer composite manufacturing, is phyllosilicates, such as MMT, vermiculite (Ver), Sep and bentonite. The FR mechanism of nanoclays is related to their layered structure, which acts as an intumescent barrier that hinders heat and mass transfer through the matrix and catalyses char synthesis of celluloses due to the metal ions in their structure [85]. Yet, upon heating, nanoclay particles accumulate on the surface of the composite, protecting bulk materials from external fire sources [33,86]. Mixing a water-soluble cellulose-based polymer with a nanoclay is normally favourable due to the polar nature of both components. Typically, clay-containing NC-based hybrids are produced by mixing their aqueous suspensions and applying casting or filtration. The morphology of the formed hybrid plays a crucial role in its performance. Many studies have reported that nature-inspired nacre or bone-like structures, or so-called brick–mortar assemblies, which can be formed between the reinforcing filler and the matrix, typically result in effective mechanical and barrier properties. Diffusion processes in the composite dramatically decrease or even blocked when particles are fully exfoliated throughout the matrix. At high dispersion of the nanosized material, high transparency of the film/coating can be achieved, which significantly expands their applicability. From a mechanical performance viewpoint, matrix-phase fibres provide strength and toughness, while clay plates provide stiffness [22].

Many research groups have demonstrated promising results by applying MMT as a fire-retarding material in nanocellulose-based free-standing films and coatings. The pioneer in this was Liu et al. manufacturing high amounts (50–89 wt%) of MMT-containing NFC nanopaper [87]. The prepared hybrid did not support any flame upon removal of the flame source, even at the lowest MMT loading, 50 wt%. Later, Carosio and co-workers published several papers on the thermal performance of the MMT/NFC hybrid [67,85,88,89]. Earliest, it was established that 30 and 50 wt% MMT containing NFC nanopapers showed significantly increased charring and self-extinguishing behaviour [85]. The authors noticed that behind the superior fireproofing is a powerful barrier effect of highly oriented MMT platelets in the NFC continuous matrix (brick-mortar structure) (Figure 2). The well-dispersed and in-plane oriented clay particles in the nanofibril matrix hinder combustion volatiles transfer and insulate the fibrils from heat. In addition, Na^+ ions on the clay surface catalyse the char-producing degradation of NFC. In the following paper, the authors studied the shielding properties of the MMT/NFC film [89]. The 100-μm thin film, containing 30 or 50 wt% of MMT, was hot pressed on an epoxy/glass fibre composite, and

subjected to an open flame source. The temperature difference between the front (coated) and back sides was 600 °C, showing the outstanding thermal protection properties of the coating. The result was the same for both 30 and 50 wt% MMT films. The fire retardancy and shielding effect of the NFC nanopaper (100 μm thickness) containing 50 wt% nanoclay were tested on wood samples [88]. The cone calorimeter test showed the effectiveness of the NFC/MMT structure (Table 5). The influence of coating on the burning scenario is shown in Figure 3. When exposed to fire, clay sheets form an expanded protective layer that delays the emission of volatiles, hindering the ignition of the coated sample. This protective barrier results in a ca. 5 min delay in ignition time for the coated sample and changes the HRR curve profile to show only one peak. Despite a slightly increased pHRR value for the coated wood sample, the total heat release is reduced by 33%. The average rate of heat emission (ARHE) was also decreased notably due to shielding effect of nanopaper. This parameter, which is defined as the cumulative heat emission divided by time, is considered one of the important fire safety factors. In another paper, researchers reported that a combination of phosphorylated NFC with MMT was more effective than neat NFC/MMT [67]. Thus, P-NFC-based coating containing only 10 wt% of MMT prevented the ignition of polyethylene (PE) substrate in cone calorimeter test. MMT was shown to be more effective compared to Sep and sodium hexametaphosphate (SHMP), which were also tested in this study. Behind the better performance is the layered structure of MMT, the ability to form a brick-mortar organization, while the rod-like sepiolite particles were randomly oriented, which led to a decrease in fire resistance properties. Creating phosphate-rich conditions, for example, incorporating SHMP, did not facilitate carbonation as might be expected. The phosphoric acid released during the thermal degradation of SHMP is reacted with C2 and C3 of P-NFC since C6 is already occupied. According to the pyrolysis mechanism, dephosphorylation at C6 leads to carbon formation, while dephosphorylation at C2 and C3 leads to the synthesis of volatiles [67].
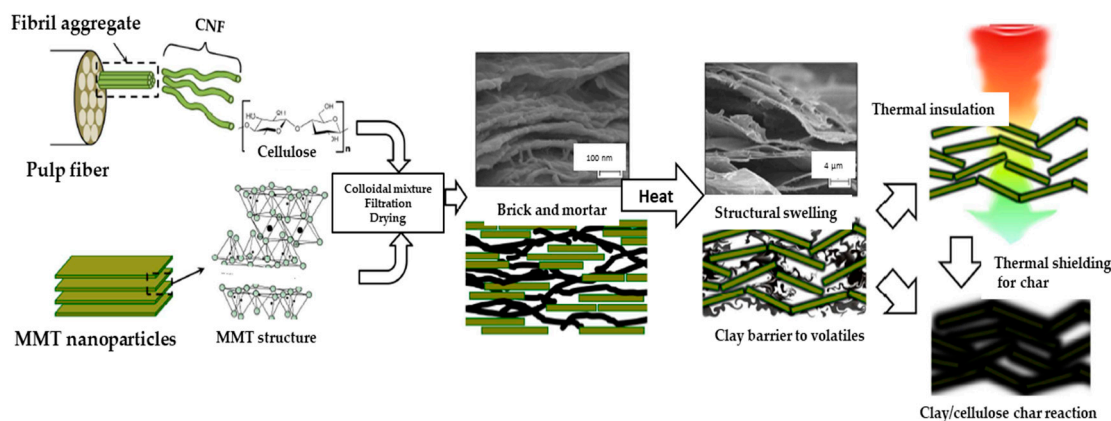

Figure 2. The schematic presentation of the brick-mortar structure in NFC/MMT nanopaper and its fire resistance mechanism (Reprinted from ref. [85] with permission from ACS Publications Applied Materials & Interfaces. Copyright (2023) American Chemical Society).

Table 5. Cone calorimeter test results for a wood sample with and without NFC/MMT nanopaper coating [88].

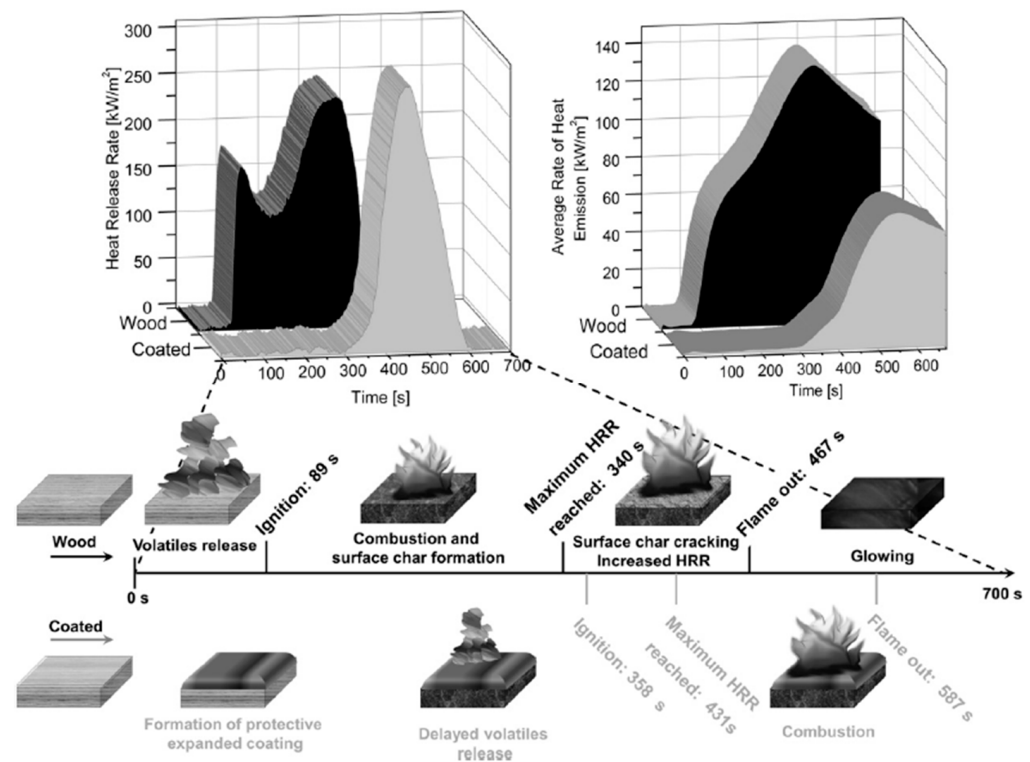| Sample	IT, s	pHRR, kW m^2	THR, MJ m^2	MARHE, kW m^2	Residue, %
Wood	89 ± 5	248 ± 9	61 ± 2	138 ± 10	15 ± 1
Coated	358 ± 58	285 ± 50	41 ± 5	74 ± 9	20 ± 2

Figure 3. Burning scenario of a wood samples (coated/uncoated) during cone calorimetry test (Reprinted from ref. [88] with permission through Copyright Clearance Center's RightsLink® service).

A promising result in transparent FR filmmaking has been demonstrated by Ming et al. [90]. Carboxylated NFC/MMT (MMT content between 5–50 wt%) hybrid films were prepared by mechanical stirring and sonication followed by evaporation. The process of hybrid preparation can be observed in its entirety in Figure 4. The FR of the films improved radically, especially at 30–50 wt% MMT. The LOI values of 30 and 50 wt% clay-containing films were about 66% and 97%, respectively; in the vertical flame test, both films were extinguished immediately after flame removal. Along with fire retardancy, the fabricated nanofilms had high optical transmittance, 90% transparency even at 50% MMT. The high FR performance of the films was attributed to the high dispersity and relatively low aspect ratio of the clay nanoparticles.

Previous examples have described batch mixing clay with a cellulose substrate, while Qin et al. used a lbl deposition technique to synthesise an NFC/Ver fireproof coating [91]. To create an electrostatic interaction with the anionic vermiculite, the NFC was functionalized with a suitable cationic surfactant. The 5–20 bilayer films, formed from a 0.2 wt% solution of NFC and a 70 wt% Ver suspension, with thickness from ca. 50 to 180 nm, were transparent at any thickness. Along with excellent O_2 barrier properties, the NFC/Ver films were also stable for fire suppression. Thus, 2–4 bl nanocoated onto polyurethane PU foam formed an effective flame barrier, which prevented the foam from melt dripping.
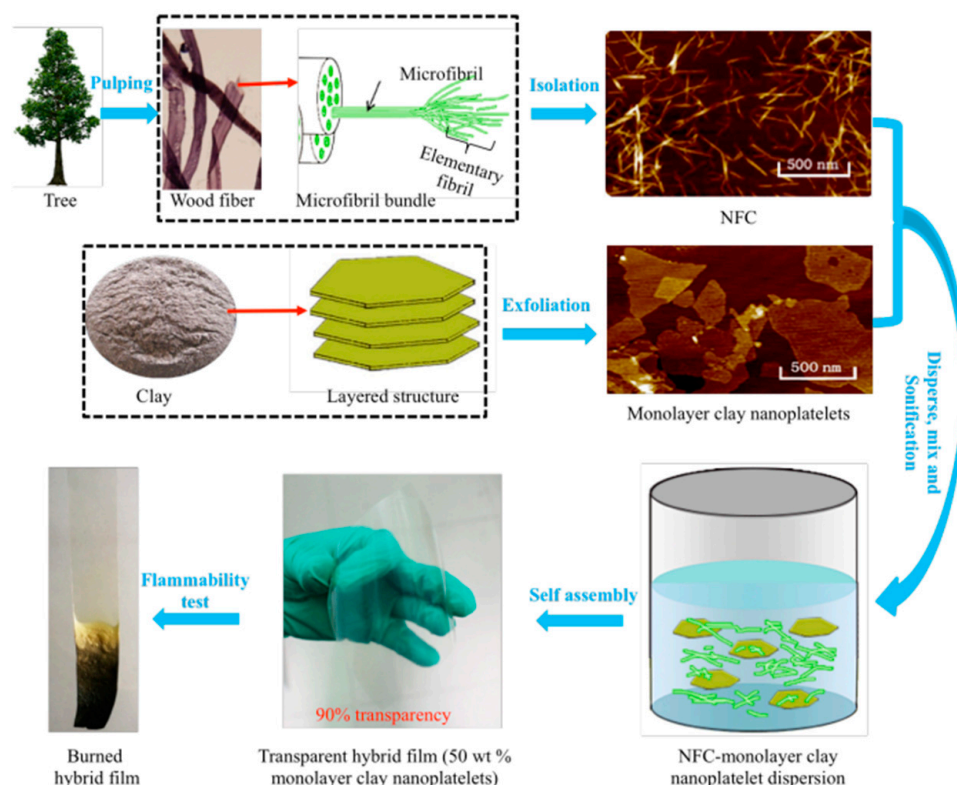
Figure 4. Schematic presentation of the preparation of highly transparent NFC/clay hybrid film with self-extinguishing behaviour (Reprinted from ref. [90] with permission from ACS Publications Langmuir. Copyright (2023) American Chemical Society).

3.2. 2D Carbon-, Black Phosphorus-, and MXene—Based Nanomaterials

EG is an intumescent FR additive that forms a worm-like structure when burned and builds a thick barrier to hinder the transfer of flammable volatiles. Santos and co-workers prepared a flame-retardant coating composed of MCC and expandable graphite [92]. The cellulose showed excellent substrate properties for the graphite due to its outstanding adhesive properties. The exfoliated reassembled graphite (ERG) particles were an effective barrier to oxygen's access to the underlying materials. A wood sample coated with a layer of MCC/EGR achieved Class A2, the highest possible class for combustible materials, according to the ISO 1182 standard [93].

In a separate work, Miao et al. used graphene oxide to modify MCC [94]. The thermal properties of the MCC/GO composites were tested by TGA and showed a significant increase in mass residue from 12% for neat MCC to ca. 50% for MCC/GO at 800 °C. Such changes were attributed to the barrier effect of the well-dispersed GO sheets as well as carbonisation-catalysing effect of sulfuric acid, which was utilised as a medium during the synthesis of the composite [95].

Zhang et al. developed a novel fire-retardant fire alarm sensor/film based on soybean protein, sisal MCC, citric acid (CA), and graphene nanosheets (GN) [96]. The GN dispersed in the film acted as a physical barrier to ignition and as a support skeleton that maintained the original shape of the film when on fire. A mechanically robust and fireproof coating made up of GO, P-NFC, and tannic acid (TA) (GO/TA/P-NFC in phr ratio 1/0.5/1) was synthesised by Cao and co-workers [97]. Fire retardancy was achieved through the combined effect of all the ingredients. Thus, TA and phosphorylated cellulose fibres contributed to the char formation. In addition, the TA catechol groups acted as reactive radical scavengers, and the phosphorus-based parts of NFC were reactive P_xO_y sources. The GO sheets served as a support for the P_xO_y nanoparticles and also protected them from degradation, accounting for the overall FR protection mechanism of the nanohy-

brid. The synthesized film was tested in a fire alarm and showed high sensitivity and flash response to temperature changes. The hybrid was also tested as an FR coating on PU foam, demonstrating its excellent performance.

Qiu et al. manufactured a mechanically strong and fire-resistant film combining black phosphorus (BP) and NFC [98]. Like graphene, BP belongs to the 2D family of materials and is characterized by thermal, chemical, and mechanical stability. The self-assembly of 2D BP and 1D NFC into a brick-mortar structure resulted in a significant decrease in pHRR and THR compared to pure cellulose. The flame retardancy of layered BP was due to a physical barrier to burning volatiles escaping from the cellulose, while the thermal oxidation of BP led to the synthesis of various PO_x substances and phosphoric acid, which in turn catalysed the carbonization of cellulose and the formation of stable char.

Xie et al. manufactured a fire-resistant coating based on ureido pyrimidinone (UPy)-functionalized hydroxypropyl methylcellulose (FC) and graphene [99]. The brick-mortar structure was formed by the co-assembly of FC molecules and GO nanosheets due to multiple H-bonds between cellulose UPy groups and O-containing moieties of GO. Single 1-µm-thick $FC/GO_{40wt\%}$ coatings on substrates, wood, PP, or PU foam, increased their LOIs and led to self-extinguishment. The fire retardancy of GO/FC was attributed to the effective barrier to oxygen and heat transfer. Moreover, the acidic groups of the fire-exposed GO sheets catalysed the dehydration and carbonization reactions of the cellulose, which facilitated the formation of chars. In addition, mechanically induced cracks on the surface of the coatings showed a self-healing phenomenon when placed in a wet environment (90% relative humidity) for 24 h. Water-induced rearrangement of cellulose molecules and GO sheets and recombination of H-bonds were observed after water evaporation.

Zeng et al. synthesized a multifunctional nanocoating (MFNC) for fire alarm detection and effective fire protection [100]. This coating was fabricated by combining $Ti_3C_2T_x$ (MXene), MMT, and UPy-containing cellulose (UPC) via layer-by-layer deposition. Excellent fire retardancy was achieved due to the barrier effect and the catalytic carbonisation of MMT and MXene. Thus, the LOI of a wood sample coated with eight layers of MFNC increased to 40% and reached a V-0 rating (UL-94). Microcombustion calorimetry showed that the HRR decreased by ca. 20% compared to uncoated wood. Water-induced self-healing of the synthesised layer was demonstrated.

The unique properties of nanomaterials are widely exploited in the development of new materials and technologies. They also show potential for applications in the flame retardancy field. This section summarised the achievement of nanocellulose-based FR coatings, in which nanoclays play a leading role. The layered structure of nanoclays creates barriers that prevent heat and fuel from reaching the substrate. In particular, the assembly of de-wetted nanoclay particles into stacked structures due to ablation of the polymer under heat makes the diffusion barrier more effective [85]. Char formation is also catalysed by clay due to the presence of Brønsted (–OH and SiOH)–Lewis (Al^{3+}, Fe^{2+}, Fe^{3+}) dual acid sites on the clay lattice. With external heat flux, these acid sites can accept single electrons from donor molecules with low ionization potential, coordinate organic radicals or abstract electrons from vinyl monomers, leading to the crosslinking of polymer chains [86]. Notably, using nanoadditives enables the processing of multifunctional high-quality materials. Thus, in many research papers, the inclusion of a nanoscale filler resulted in greater flame retardancy as well as better mechanical performance. In the case of using graphene oxide in fire sensing films/coatings, fire retardancy is accomplished by its rapid reduction into high-conductive graphene under a flame. Such a conversion allows an alarm to be triggered within seconds. The use of nano-sized fillers also allows to production of transparent films/coatings, which is an additional advantage of naturally transparent nanocellulose-based substrates.

The main disadvantage of nanosized fillers is their tendency to form aggregates due to high surface energy. To achieve a stable colloidal suspension of nanoparticles, vigorous mechanical steering, sonication, or centrifugation is typically necessary. Additionally, some

additives can be too expensive, such as carbon-based, graphene, and EG, which are mostly used in demanding and small-scale applications.

4. Potential of Lignin and Chitosan in Cellulose-Based FR Coatings

Owing to its intrinsic fireproof functionality, lignin is often used as an additive in FR formulations, particularly synthetic polymers [101–103]. The potential for lignin in fire-retarding nanocellulose-based films has been observed by Zhang et al. when they compared pure cellulose and pre-phosphorylation lignin-containing cellulose fibres for NFC processing [14] (see Section 2). Zheng et al. compared two types of lignin, kraft, and sulfonated kraft, as fire retardant additives for MFC-based coating [104]. In addition, other FR systems, that is, a nanoclay, a commercial EG and a synergetic fire retardant (50% ammonium sulfate, 10% ammonium polyphosphate (APP), and 40% Al(OH)$_3$), were tested. The thermal stability and flammability of these coatings were evaluated by mean TGA and cone calorimetry. Selected results are shown in Table 6. The MMT-containing coating had the best values, despite the MMT/MFC coating being ten times thinner than all other coatings tested here. Amongst the lignin-containing samples, the presence of sulfonated kraft lignin decreased pHRR significantly and increased mass residue (TGA). The FR properties of sulfonated kraft lignin relate to the higher content of sulfur, 4–5%, while kraft lignin is limited to 2–3% [105]. The FR property of a coating containing EG is due to the formation of intumescent worm-like char at 160–170 °C, which significantly prolonged the IT and reduced the pHRR and THR. The synergistic FR improved the FR of the sample because of the cellulose charring due to the acid catalytic dehydration induced by ammonium sulfate and ammonium polyphosphate, diluting effect of the evolved NH$_3$, as well as the formation of Al$_2$O$_3$ and water vapour due to Al(OH)$_3$ decomposition, i.e., the proposed effect of commercial FR according to its composition.

Table 6. FR parameters of coatings containing different FR additives [104].

Sample	IT, s	pHRR, kW m^{-2}	THR, MJ m^{-2}	TGA, wt%/800 °C
Reference, no coating	12 ± 4	120 ± 6	10 ± 1	15 ± 1
MFC, 100%	18 ± 1	127 ± 9	11 ± 1	22 ± 1
Sulf. kraft lignin (10%) + MFC	12 ± 1	85 ± 4	8 ± 2	52 ± 0
Kraft lignin (10%) + MFC	14 ± 2	127 ± 8	11 ± 1	40 ± 2
Nanoclay (10%) + MFC	no ign.	5 ± 1	0.4 ± 0.1	87 ± 0
Synergistic FR (10%) + MFC	34 ± 2	47 ± 6	4.2 ± 0.2	45 ± 3
EG (10%) + MFC	26 ± 8	47 ± 1	7 ± 0.4	74 ± 2

The synergistic effect of lignin as a source of charring and boron-containing FR (borax) as a char-former on NFC has been explored by Tong et al. [106]. Cone calorimetry showed that this combination resulted in reducing pHRR, THR, and total smoke production (TSP) by 79%, 56%, and 99%, respectively, compared to the neat NFC sample. The residue yield increased up to 43 wt%, while neat NFC and samples containing only lignin or FR, were left 4, 15, and 38 wt%, respectively. The presence of lignin or FR improved the LOI from 19.9% for neat to 23.3 and 50.9% for lignin-containing and FR-containing samples, respectively; samples containing both components, lignin and borax, had an LOI of 43.9%. Dos Santos et al. have reported that wood impregnated with an emulsion of kraft lignin had a delayed IT, from ca. 12 s to ca. 26 s, for untreated and treated samples, respectively [107]. The flame and ember times increased, whereas the weight loss decreased from ca. 34% to ca. 27%.

Chitosan is another bio-based polymer that shows excellent fireproofing functionality. The high charring ability of chitosan is accomplished by the blowing effect evaporating N$_2$, which originates from the amino group of the chitosan backbone. Uddin et al. have reported that a combination of NFC and CH resulted in a thermally stable, self-extinguishing film, which left up to 86% mass residue in a vertical flame test [108]. In another work, Pan et al. used phosphorylated MCC and chitosan as components for a coating to protect cotton fabric using lbl coating [109]. In this technique, the fabric piece was alternately dipped

into CH (cationic) and P-MCC (anionic) solutions. The vertical flame test showed that fabric coated in 20 bilayers (bl) of CH (0.5%)/P-MCC (2%) was self-extinguishing after the flame was removed: 90% of the fabric was preserved. The mass residue in the TGA increased from 10% to ca. 40% for pure and 20-bl samples, respectively. Carosio et al., and Köklükaya et al., have used CH as a component for multi-layered FR coating for NFC-based foams [110,111] (see Section 5).

Currently, the most utilised charring agent in the fire retardants field/intumescent system is pentaerythritol, which is produced from fossil fuel sources. From an environmental perspective, using natural char-forming compounds such as lignin, chitosan and starch is of interest in the development of modern FR technologies. Due to its polyaromatic structure and high carbon-to-oxygen ratio, lignin is a high char-yielding polymer. Approximately 57 wt% of its initial mass is transformed into char at 600 °C (in N_2 atmosphere) [112]. To further improve its fire retardancy, lignin can be modified or used with a synergistic component [104,113]. However, several properties of lignin can be taken into account for FR material development. The main drawback of lignin is its dark colour, which can limit the application field of lignin-based formulations. Another potential difficulty is its polyphenolic structure, which screens its own hydrophilic moieties, resulting in poor compatibility with cellulose. Chitosan, which is derived from natural chitin by alkaline deacetylation, can be used as a carbon-forming agent due to its carbohydrate structure with abundant OH and NH_2 groups in the backbone. According to TGA, neat chitosan forms ca. 40 wt% [114] of residue in an inert atmosphere and ca. 20 wt% in air [115]. Chitosan is often utilised in multi-layered coatings through lbl assembly due to its high positive charge density, induced by the protonation of NH_2 (at low pH) and high solubility. Chitosan is becoming increasingly popular as a bio-based FR material in textile treatment and different composite formulations, but its price may limit its large-scale commercialization [116].

5. Aerogels and Foams with Improved Fire Resistance

Aerogel design and production is another field where nanocelluloses can be utilised as substrates or modifying agents. The high porosity and light weight of aerogels make them attractive materials for many applications, including thermal insulation. However, unlike mineral-based materials, bio-based aerogels are highly flammable, significantly restricting their application. Two approaches have been used for cellulose-based aerogel FR design: incorporation of FR additive during aerogel synthesis or deposition of an FR coating on the aerogel surface.

5.1. Effect of Cellulose Grade/Modification

Niu et al. have used the phosphorylated grade of MCC for aerogel processing [117]. MCC was treated with a H_3PO_4/P_2O_5/triethyl phosphate/1-hexanol mixture for 48 or 72 h. TGA showed that the char residue increased significantly, from 2.2% for neat MCC to 36.6% and 37.1% for P-MCC (48 h) and P-MCC (72 h), respectively. The LOI reached 42.5% and 54.5% for P-MCC (48 h) and P-MCC (72 h), and both samples received V-0 ratings in the UL-94 test. The P-MCC based samples had flameless burning with very low pHRR in the cone calorimetry. Remarkably, aerogel fabrication was optimised with added phosphorous due to improved dispersion stability and enhanced gelation.

Zhu et al. have used chemithermomechanical pulp (CTMP) to develop lignocellulosic nanofibrils (LNFC) using sulfamic acid- and urea-composed deep eutectic solvents (DES) [118]. Compared to dissolving pulp, CTMP retains significant amounts of hemicelluloses and lignin. It has been demonstrated that the LOI of aerogel processed from LNFC reached 35.3%, surpassing the self-extinction value of 26–28% [30], which was also demonstrated by UL-94 test. In the TGA, the mass retention increased to 35% for LNFC, whereas the pristine CTMP sample retained only 7.9%.

5.2. Effect of Nanoclays, Metal-Containing, Graphene Oxide, Hydroxyapatite, Metal-Organic Frameworks (MOFs), and Conventional FRs

Donius et al. have produced an NFC/MMT (50/50 wt% ratio) foam with significant fire retardancy performance [22]. The presence of MMT decreased notably the degradation rate and increased the char residue up to 60%, as determined by TGA. Later, Carosio et al. prepared an NFC/xyloglucan/MMT (27/40/33 wt% ratio) composite foam where xyloglucan (XG) was used as a strengthening binder due to its affinity to both cellulose and MMT [119]. Xyloglucan provides good interactions with MMT in the presence of monovalent ions in nanoclay structure (e.g., Na$^+$). On the other hand, XG and NFC have high affinity due to H-bond interactions. The fabricated ternary foam by freeze-casting method had high porosity (98.5%) and a brick-mortar cell wall structure where a matrix consisting of NFC and XG-coated MMT platelets acted as platelet reinforcement (Figure 5a). The foam demonstrated self-extinguishing behaviour immediately after the ignition source was removed, whereas polyurethane (PU)-made foam burned completely (Figure 5b). In the cone calorimeter test, the fabricated foam had significantly lower heat release and smoke production parameters compared to conventional rigid PU foam (Figure 5c). The flame resistance test showed that the fabricated foam could prevent flame penetration resulting in a temperature drop at unexposed to flame side (Figure 5d). In another work, Wang and Sánchez-Soto demonstrated the combined fireproof effect of MMT and APP in an aerogel made of recycled cellulose fibres and carboxymethyl cellulose [120].
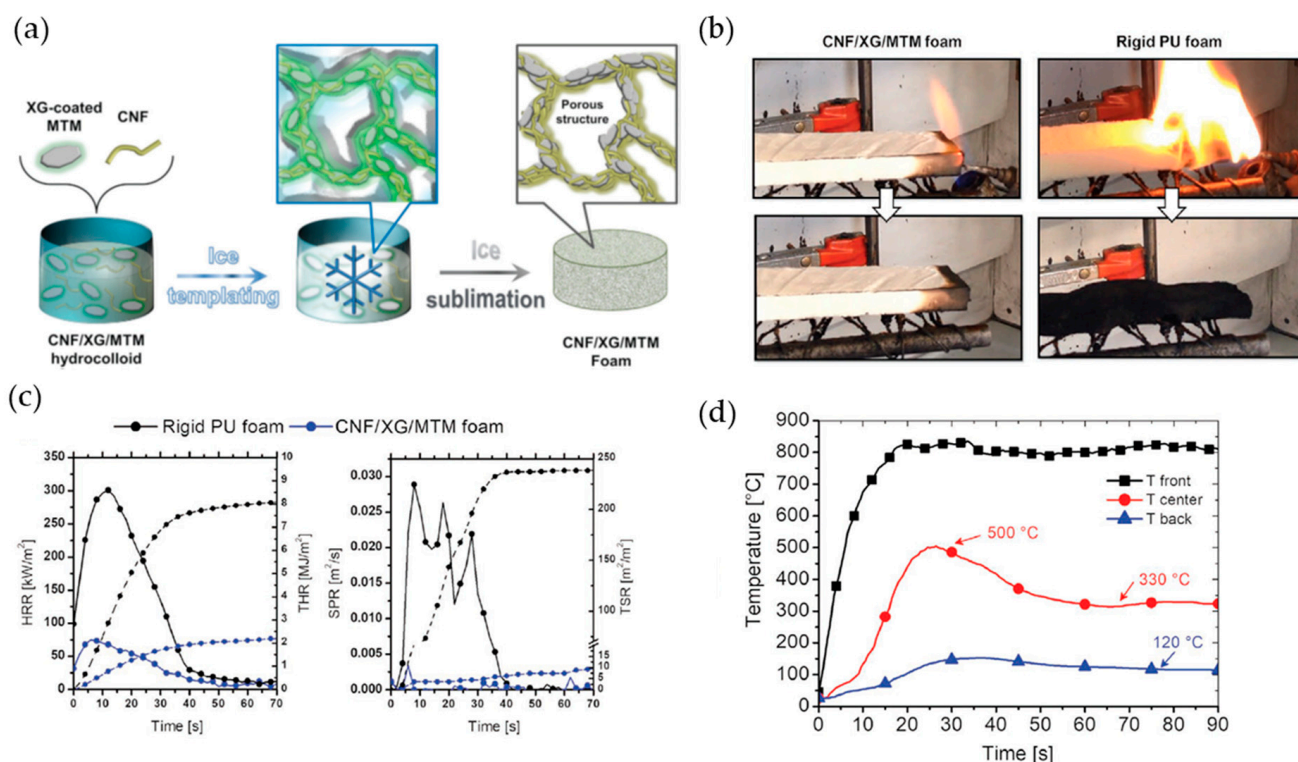

Figure 5. (**a**) Schematic presentation of NFC/XG/MMT foam synthesis; (**b**) flammability test results; (**c**) cone calorimeter test; (**d**) average temperature profile records in flame resistance test. (Reprinted from ref. [119] with permission from Wiley-VCH GmbH through CCC RightsLink).

Han et al. fabricated a flame-retardant cellulose aerogel from waste cotton fabric by in situ synthesis of magnesium hydroxide nanoparticles (MHNPs) [121]. The combustion velocity decreased from 5 mm s^{-1} for the neat cellulose aerogel to 0.8 mm s^{-1} for the aerogel modified with MHNPs, and self-extinguishing within 40 s. Similarly, He et al. have synthesised fire-resistant cellulose aerogel containing aluminium hydroxide nanoparticles (AHNPs) [122]. According to the MCC test, the time to ignition was extended from 17 s

for the neat foam to 26 s for the AHNP-containing foam. Also, the THR, pHRR, and residue parameters of the hybrid aerogel were superior to those of the neat sample. Apart from the fireproof properties, the mechanical performance of foams containing Al and Mg hydroxide nanoparticles was also improved. Fan et al. have incorporated AlOOH into a NFC aerogel, resulting in at least 60 s of fire resistance [123]. The sol-gel technique used by Yuan et al. to synthesise $Al(OH)_3$/cellulose hybrid aerogels with improved FR properties [124]. Thus, 56–67 wt% Al hydroxide (AH)–containing cotton cellulose-derived aerogel showed a significant reduction in THR and pHRR, as seen in Table 7. The same authors have also prepared a cellulose–silica composite aerogel. The aerogel with high silica content (>34%) has high light transmittance and self-extinguishing behaviour [125].

Table 7. Micro-scale combustion calorimetry results of regenerated cellulose aerogel and cellulose/AH nanocomposite aerogels [124].

Sample	THR, kJ g^{-1}	pHRR, W g^{-1}	T_{pHRR}, °C	R,%
NFC	11.3	294	351	14
NFC/AH (56 wt%)	2.0	51	240	50
NFC/AH (67 wt%)	1.7	24	247	60

Farooq et al. have prepared a NFC/sodium bicarbonate (SBC) aerogel using the freeze-drying method [126]. All composites containing different amounts of $NaHCO_3$, 10–40 wt%, showed slow flameless glowing, charring and self-extinguishing behaviour. Thus, the average combustion velocity of the NFC/SBC hybrid in the horizontal combustion test was 5.84 cm s^{-1}, whereas the pure aerogel was fully burned in <1 s. The optimal combination to achieve the desired flame retarding properties was 20 wt% $NaHCO_3$-NFC. The mechanism of SBC was described as follows: (i) SBC absorbs heat and (ii) decomposes, liberating CO_2 and H_2O, which dilute or obstruct the O_2 supply to the burning surface. In addition, the vaporisation of water consumes energy in the system. Yang et al. have used MoS_2 nanoparticles to improve the fire resistance of NFC-based foam [49]. The TGA test showed that NFC/MoS_2 aerogel left behind up to 46 wt% residue and self-extinguished in the vertical flame test. The LOI was 34.7%.

Several research papers demonstrate the potential of using hydroxyapatite (HA) in fireproof thermal insulating foams. Guo et al. have used HA nanofibers to improve NFC foam fire retardancy, with NFC:HA mass ratios of 1:2, 1:1 and 2:1 [127]. TGA showed increased mass residue up to ca. 70% at the highest HA (NFC:HA = 1:2 ratio) loading. Cone calorimeter analysis detected a significant decrease in pHRR, 91%, with respect to the pure NFC foam sample. Also, the nanocomposite was self-extinguished in the burning test. Yang et al. reported that the hybrid composed of MCC/HA (50 wt%) did not ignite but smouldered, leaving char residue close to the theoretical value of 48 wt% [128]. The hybrid showed a significant reduction in pHRR and TSP, ca. 94%, and more than 74%, respectively, when compared to pure MCC. The addition of HA did not affect the thermal insulating properties; however, it increased the hybrid's brittleness. A lightweight NCC/HA hybrid with improved mechanical and thermal stability was developed by Huang et al. [129]. The hybrid structure mimicking natural bone structure was synthesised using simulated body fluid. During the freeze-casting, NCC coated with HA nanoparticles forms a porous structure while the acidity of the ambient media is used to control the amount of HA content in the final product. The presence of a high amount of HA, up to 47 wt%, significantly increased the thermal stability of the material.

Ghanadpour et al. have combined phosphorylated NFC and Sep nanorods, (P-NFC/Sep equal to 60%/40%) to manufacture freeze-cast foam with excellent insulating and fireproof performance [130]. Several factors were behind the fireproof performance the synthesized foam: (i) intimate contact between nanosized Sep fibres and P-NFC; (ii) the honeycomb structure; (iii) intrinsic FR of phosphorylated cellulose and (iv) the capability of sepiolite to form a heat-protective intumescent barrier. Figure 6 shows flammability testing results, cone calorimetry, and thermal insulating properties measurement. The fabricated

foam was self-extinguished after flame removal (Figure 6a). In the cone calorimetry, the foam structure did not change after a very short ignition period and a few seconds of glowing, as shown in Figure 6b. As a result, the pHRR of the hybrid foam was only 34 kW m^{-2} (Figure 6c) which is significantly lower than that of commercially available flame-retardant phenolic foams (70–100 kW m^{-2}). In addition, the prepared foams were able to withstand the penetration of flame (Figure 6d) due to a temperature drop across foam of more than 600 °C (Figure 6e) which is sufficient for only 10 mm-thick foam.
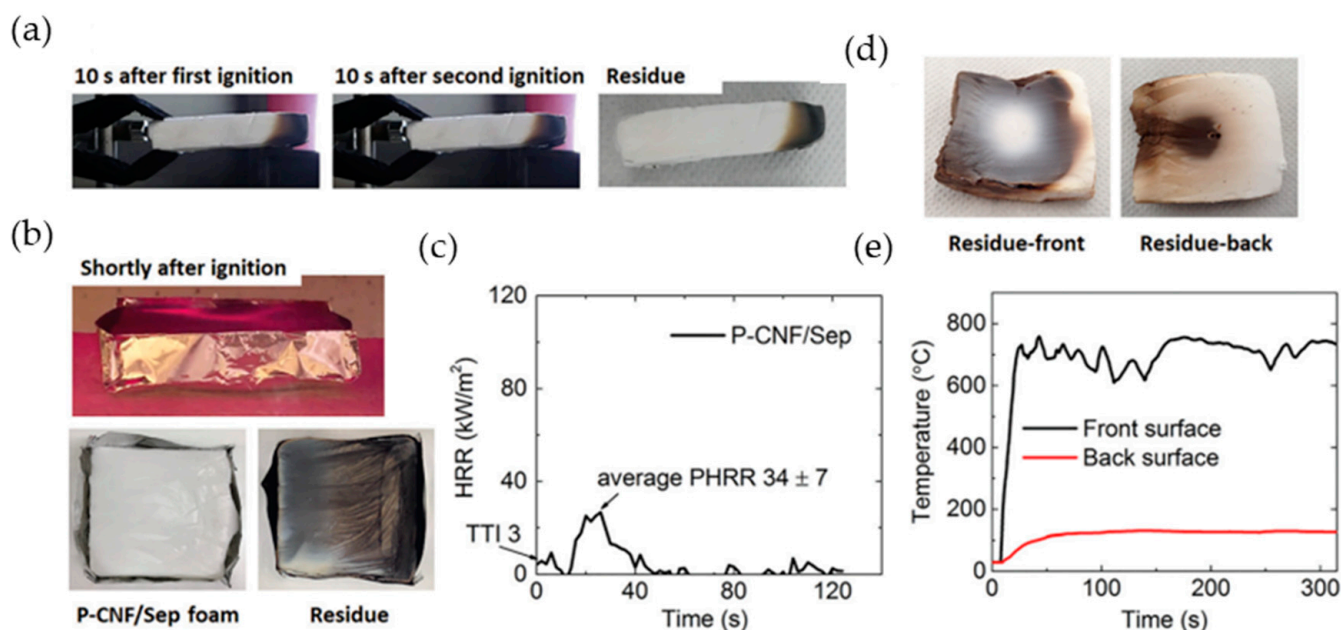
Figure 6. The P-NFC/Sep foam testing results: (**a**) flammability test; (**b**) cone calorimetry testing photographs; (**c**) the HRR curve; (**d**) methane torch flame penetration test result; (**e**) temperatures measured on front and back sides during flame penetration test (Reprinted from ref. [130] with permission from the Royal Society of Chemistry).

Wicklein et al. synthesised NFC-based foam which was modified with 10 wt% graphene oxide, 10 wt% Sep, and 3 wt% boric acid (BA) by ice templating [131]. TGA showed that the GO, Sep, and BA-containing foam left up to 55% carbon-rich residue at 900 °C. The LOI achieved 34%, which is significantly higher than the LOIs of commercial flame retardant-containing polymer-based foams, i.e., 22–25%. Cone calorimetry showed that the nanocomposite foam did not properly ignite but remained between smouldering and ignition, and the pHRR was 25% lower than that of the NFC. The authors reported extremely low thermal conductivity of the synthesised foam, 15 mW m^{-1}K^{-1}, which is as half as low commercial expanded polystyrene (EPS) foam (=35 mW m^{-1}K^{-1}). In another work, the same group has demonstrated the significance of the fabricated composite structure [132]. The high degree of crosslinking between the borate and the cellulose substrate resulted in the higher performance of the manufactured foam. The better crosslinking of the boron moiety with cellulose substrate is favourable for cellulose charring, where BA acted as a char former facilitating graphitization of NFC. The combustion resistance was also improved by Sep, which formed a silicate-rich layer on the burning surface. In another study, Cheng et al. used boron-based FR and zinc borate (ZB) to achieve fire retardancy of NFC foam [133].

Guo et al. have used red phosphorous hybridized graphene (PGN) nanosheets for manufacturing fire-resistant NFC-based foam [134]. The pHRR and THR of PGN-NFC hybrid foam decreased by 94% and 56%, respectively, compared to neat NFC item, while the char residue increased up to 31 wt% in contrast to neat NFC which decomposed almost completely to volatiles leaving only 5% solid. In an open flame test, the hybrid foam was self-extinguished.

Recently, MOFs-derived FRs have been explored as a novel additive in synthetic polymeric materials and have demonstrated applicability in cellulose-based substrates [53–56]. MOFs can be described as crystalline porous hybrids built up from metal ions or clusters and organic ligands. Several MOFs based on Zeolitic Imidazolate Frameworks (ZIFs), Material Institute Lavoisier (MILs), University of Oslo (UiO), are applied to design novel functional hybrids [56]. The most commonly used metal cations in MOFs are divalent transition (Zn^{2+}, Cu^{2+}, Co^{2+}, Ni^{2+}), trivalent (Cr^{3+}, Al^{3+}, Fe^{3+}), and four-valent metals like Zr^{4+} and Ti^{4+} [135]. Notably, simple mixing MOFs and polymers does not result in a composite with unique properties, while hybridisation or template-assistant synthesis, in which rigid MOF crystals are grown on a flexible substrate leads to the formation of polymer@MOFs composite with significantly improved functionality, including enhanced fire resistance. Nabipour and colleagues have compiled data on metal-organic frameworks used for the flame retardation of polymers, which is presented in their review article [53]. The FR mechanism action of MOFs can be described as follows: (i) upon heating, MOFs decompose to form a metal oxide, which covers the substrate and protects it from thermolysis; (ii) MOFs absorb gases and smoke; (iii) during decomposition, MOFs release non-flammable gases, which dilute fuel gas whereby hindering burning and heat release; (iv) suppression of combustion, in turn, results in enhanced charring. Currently, several papers report the use of MOFs as flame retardants for cellulose-based materials. Zhou and co-workers synthesized four different NFC@MOFs through a procedure illustrated in Figure 7a. They first ion-exchanged metal ions with carboxylated NFCs. Next, they modified the NFCs' surface by adding some amount of surfactant polyvinylpyrrolidone (PVP). Afterwards, they introduced metal salts and organic ligands. The films created from NFC@MOFs (with around 25 wt% of MOFs) were highly transparent and flexible, as shown in Figure 7b. SEM micrographs revealed homogeneously stacked NFC@MOFs nanofibers while NFCs were uniformly wrapped by continuous MOF layers, as shown in Figure 7b,c. TGA analysis indicated that films made from NFC@MOFs nanofibers were more thermally stable compared to those made from pure NFC. The decomposition temperature was higher, and the mass residue increased compared to the neat NFC-produced material [55]. The same author used alumina-based MOFs for the fabrication of aerogel from NFC@Al-MIL-53 to improve its insulating and FR performance [136]. The resulting foam demonstrated low thermal conductivity and self-extinguishing behaviour. Additionally, the designed aerogel exhibited moisture resistance and superelasticity. Another study conducted by Nabipour et al. displayed that cellulose@ZIF-8 aerogel thermal and mechanical performance was improved significantly compared to the host cellulose-based one [54]. It was reported that pHRR reduced from 128 W g^{-1} to 63 W g^{-1} for neat cellulose-made aerogel and cellulose@ZIF-8, respectively. Also, the aerogel was self-extinguishing and LOI achieved 42%.

The advantage of this technique is that a variety of different combinations of metal moieties and organic ligands can be utilized to create MOFs with specific functionalities, porosity and geometric features (0D, 1D, 2D, and 3D). However, despite the obvious advantages of MOF-based material, there is still a need for fundamental research to expand knowledge of MOFs action and their potential applications. Additionally, the high cost of ligands remains a significant drawback of MOFs, which can limit their commercial viability [56].
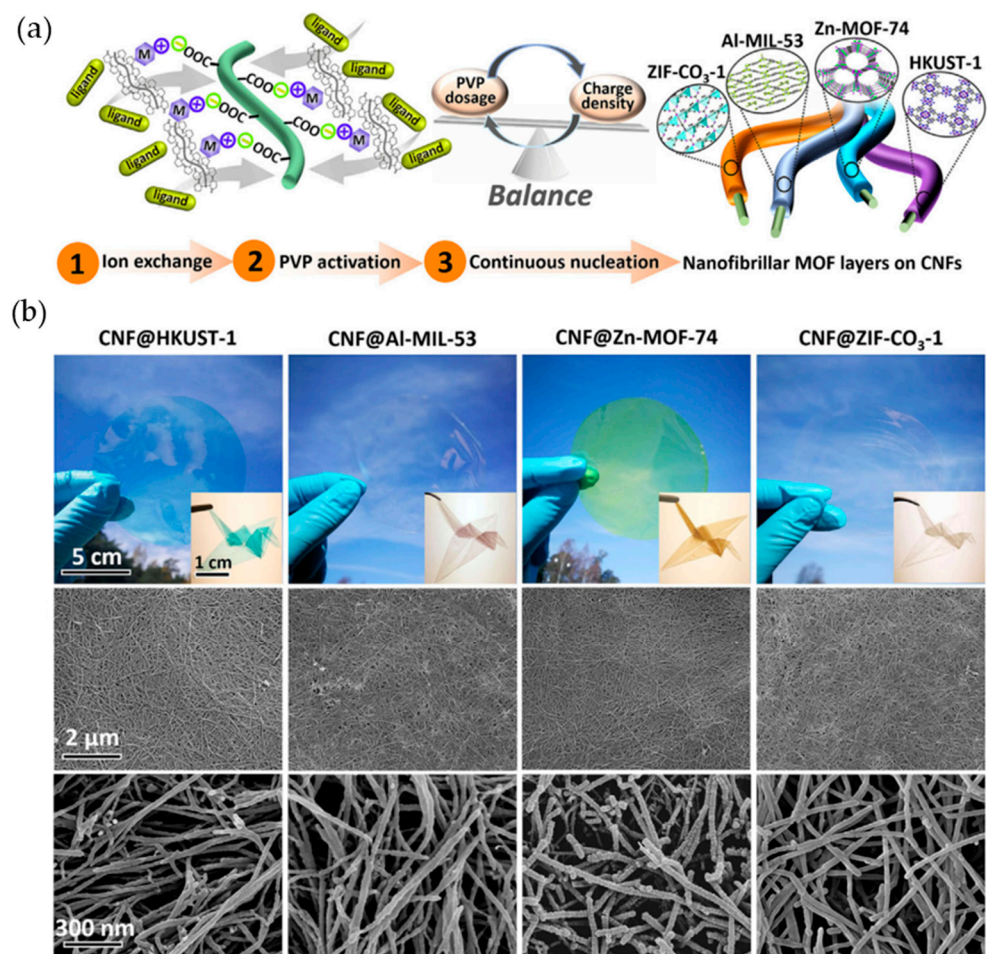
Figure 7. (**a**) Schematic presentation of the synthesis procedure of the NFC@MOF hybrids. (**b**) photographs and SEM-images of NFC@MOFs nanopapers (Reprinted from Ref. [55] with permission through Copyright Clearance Center's RightsLink® service).

5.3. Layer-by-Layer Deposition of FR Coatings, Effect of Chitosan and MMT

The high porosity and high surface area of aerogels allow for their modification using the lbl deposition technique. Köklükaya and co-workers have improved the fireproof properties of NFC-based aerogels by the deposition of nanometer thin film composed of cationic chitosan, anionic poly(vinylphosphonic acid) (PVPA), and anionic MMT nanoclays [111]. The five coatings, each composed of CH/PVPA/CH/MMT, were homogeneously placed on the substrate without changing the pore structure, while the mass was increased by 19%. At optimal concentrations of components, these coatings resulted in self-extinguishing of the aerogel in the flammability test and remarkably higher residue compared to the untreated sample in TGA. Carosio et al. covered PU foam with CH/phosphorylated NFC film by the lbl technique [110]. The coating procedure is schematically displayed in Figure 8. The open-cell PU foam piece was alternatively dipped into chitosan (positive) and phosphorylated cellulose nanofibrils (negative) solutions. Between solution changes the foam was rinsed with water. Cone calorimetry testing under 35 kW m^{-2} heat flux showed that 5-bl CH/P-NFC coating accounting for only 8% of added weight reduced the combustion rate by 31% and prevented the dripping of foam.
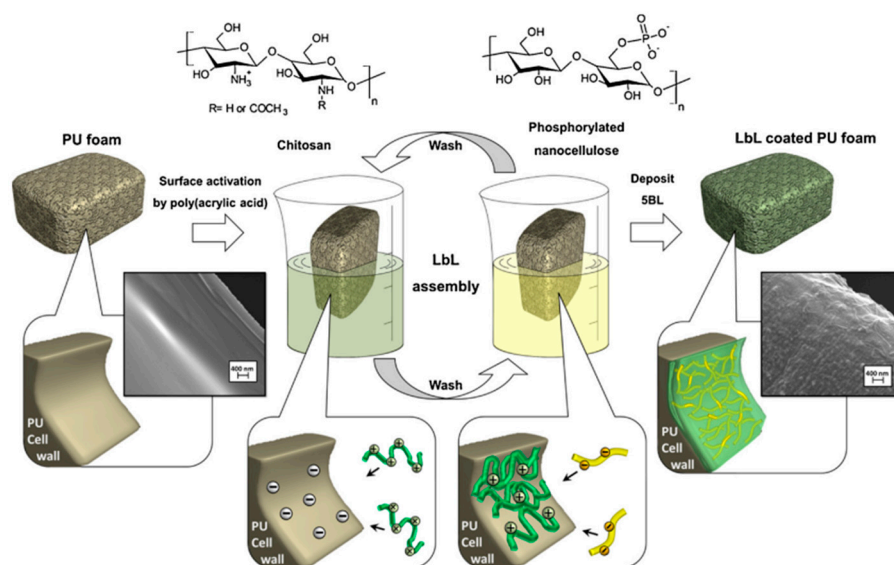
Figure 8. Schematic presentation of layer-by-layer deposition of cationic chitosan and anionic P-NFC on PU foam with washing between each adsorption step (Reprinted from ref. [110] with permission from Elsevier through Copyright Clearance Center's RightsLink® service).

As it was established, layer-by-layer deposition has proven to be a simple and effective technique for developing functional coatings. However, a possible obstacle for large-scale operations is that numerous layers must be assembled to achieve the desired effect. In addition, the amount of positively charged substances that can be used for fire-resistant coatings is very limited. Thus, the main cationic material currently used for FR lbl films is chitosan.

5.4. Alginate- and Tannin-Based FR Foams

Alginate is a polymer obtained from seaweed plants that has recently been researched because of its interesting features, including biocompatibility, biodegradability, easy crosslinking, and resistance to fire [137]. Berglund et al. have manufactured foam from NFC extracted from alginate-rich seaweed, A-NFC. The A-NFC foam was prepared by freeze-drying and was post-crosslinked with $CaCl_2$ [138]. According to the flammability test (UL-94), the average combustion velocities for pure A-NFC and crosslinked A-NFC were 1.2 mm s^{-1} and 0.75 mm s^{-1}, respectively, leaving behind uncollapsed shrunken char residue. The burning rate is significantly lower than that of the aerogel formed from pulp cellulose, 58.5 mm s^{-1}. The fire retardancy of the A-NFC aerogel was attributed to the inherent resistance to fire of the alginate material, which was further improved by crosslinking with $CaCl_2$.

Missio et al. have recently manufactured tannin-based foam, in which NFC was used as the crosslinking agent [139]. Using NFC (0.1 wt%) instead of formaldehyde resulted in shifting the mass loss peak to higher values, from ca. 400 °C to 420 °C in TGA. Also, the mass loss of foam exposed to flame decreased from ca. 22% to 12% for the formaldehyde- and NFC-containing foams, respectively. Moreover, the NFC-reinforced tannin-based foam was self-extinguishing, showing no ignition during several minutes of exposure to a flame.

This section presents achievements in manufacturing fire-retardant nanocellulose-based foams and aerogels. As it aforementioned, cellulose/bio-based aerogels are typically produced by freeze-drying procedure, which is simple, economical and environmentally friendly. Thus, cellulose-based aerogels are highly sustainable materials considering that cellulose itself is an unexhausted, renewable and biodegradable. Obtained aerogels are characterised by a large porosity, high specific area, and a unique 3D structure that are useful in various areas, such as adsorption, separation technology, medicine, and the construction field as insulating material. An advantage of biobased foams and aerogels is

their ability to be customized with functional additives, resulting in sustainable materials with unique properties. Thus, despite the significant organic content, even more than 60 wt%, NC-based modified foams show excellent flameproof performance [119,130,131]. In this respect, combining many useful functional properties along with the sustainable character of cellulose, ultralight NC-based aerogels and foams are considered an appealing alternative to traditional foams like PU, EPS, and glass wool [119,130,131,140,141].

6. Conclusions

The great potential of fire-resistant coatings and free-standing films/nanopapers developing based on eco-friendly nano/microcelluloses has been established in this review. To achieve a fire retardancy effect, the cellulose-based substrate is typically managed via chemical modification and/or physical mixing with fireproof additives. The basic method for cellulose modification is phosphorylation, which inhibits the formation of combustible levoglucosan and promotes char synthesis. The ever-increasing ecological issue is also reflected in the preference for fire-retarding materials for developing novel FR systems. The research papers cited in this review showed the different ways to achieve fireproof coatings. It was shown that using different approaches, by either incorporating mono additive or combining different FRs mechanisms, a self-extinguishing, V-0 rating, and smoke release suppression can be achieved.

In conclusion, there are several advantages and obstacles in the development of flame-retardant coatings derived from cellulose:

- Cellulose-based FR coatings showed promising results. Due to the presence of reactive OH groups in the backbone, cellulosic polymers can be easily modified. Phosphorylation of cellulose is an effective way to obtain an intrinsically flame-retardant grade of cellulose. The cellulosic substrate is compatible with many nanosized additives and conventional flame retardants. Unlike its counterparts, thermoplastics and thermosets, cellulose-based coatings, and films can be processed at ambient conditions.

- However, the development of NC-based coatings is mostly presented on a laboratory/bench scale. The main obstacle to large-scale commercialization remains the high cost of processing nanocelluloses, >100 USD per dry kg [142]. Decreasing the cost to <10 USD per kg (e.g., for NFC) will make nanocellulose material sustainable. This cost decrease can be achieved by increasing production capacity [142].

- One of the ways to facilitate nanocellulose production is by reducing the energy cost required for nanofibrillation. It was shown that significant energy input can be saved by using a twin-screw extruder (TSE) for cellulose processing [19]. Thus, phosphorylated NFC processing required energy consumption between 300 and 1000 kWh/t by using TSE compared to the case of using an ultra-fine grinder, with 11,000 kWh/t energy required for the manufacturing of a similar product. Alternatively, high-consistency enzymatically fibrillated cellulose (HefCel) nanocellulose grade can be processed at a high solid content (up to 25%) and 600 kWh/t energy input [80].

- Forest-derived materials have the potential to play a key role in the development of a circular economy. Nanocellulose is a particularly attractive material that could be used for coatings, free-standing films, and other applications. As technical and economic barriers are overcome, cellulosic materials could replace fossil-derived counterparts in bulk applications in the future.

Author Contributions: Writing—original draft preparation I.T.; writing—review and editing, I.T. and L.P.; supervision—L.P.; administration—A.R. and T.T. All authors have read and agreed to the published version of the manuscript.

Data Availability Statement: Not applicable.

Conflicts of Interest: The authors declare no conflicts of interest.

References

1. Dahmen, N.; Lewandowski, I.; Zibek, S.; Weidtmann, A. Integrated lignocellulosic value chains in a growing bioeconomy: Status quo and perspectives. *Glob. Chang. Biol. Bioenergy* **2019**, *11*, 107–117. [CrossRef]
2. Hubbe, M.A.; Ferrer, A.; Tyagi, P.; Yin, Y.; Salas, L.P.; Rojas, O.J. Nanocellulose in thin films, coatings, and plies for packaging applications: A Review. *BioResources* **2017**, *12*, 2143–2233. [CrossRef]
3. Trache, D.; Tarchoun, A.F.; Derradji, M.; Hamidon, T.S.; Brosse, N.; Hussin, M.H. Nanocellulose: From Fundamentals to Advanced Applications. *Front. Chem.* **2020**, *8*, 392. [CrossRef] [PubMed]
4. Oksman, K.; Aitomäki, Y.; Mathew, A.; Siqueira, G.; Zhow, Q.; Butylina, S.; Tanpichai, S.; Zhou, X.; Hooshmand, S. Review of the recent developments in cellulose nanocomposite processing. *Compos. Part A Appl. Sci. Manuf.* **2016**, *83*, 2–18. [CrossRef]
5. Moon, R.J.; Martini, A.; Nairn, J.; Simonsen, J.; Youngblood, J. Cellulose nanomaterials review: Structure, properties and nanocomposites. *Chem. Soc. Rev.* **2011**, *40*, 3941–3994. [CrossRef] [PubMed]
6. Vanderfleet, O.M.; Cranston, E.D. Production routes to tailor the performance of cellulose nanocrystals. *Nat. Rev. Mater.* **2021**, *6*, 124–144. [CrossRef]
7. Zhu, H.; Luo, W.; Ciesielski, P.N.; Fang, Z.; Zhu, J.Y.; Henriksson, G.; Himmel, M.E.; Hu, L. Wood-Derived Materials for Green Electronics, Biological Devices, and Energy Applications. *Chem. Rev.* **2016**, *116*, 9305–9374. [CrossRef]
8. Klemm, D.; Kramer, F.; Moritz, S.; Lindström, T.; Ankerfors, M.; Gray, D.; Dorris, A. Nanocelluloses: A new family of nature-based materials. *Angew. Chem. Int. Ed.* **2011**, *50*, 5438–5466. [CrossRef]
9. Sirviö, J.A.; Hasa, T.; Ahola, J.; Liimatainen, H.; Niinimäki, J.; Hormi, O. Phosphonated nanocelluloses from sequential oxidative-reductive treatment—Physicochemical characteristics and thermal properties. *Carbohydr. Polym.* **2015**, *133*, 524–532. [CrossRef]
10. Ghanadpour, M.; Carosio, F.; Larsson, P.T.; Wågberg, L. Phosphorylated Cellulose Nanofibrils: A Renewable Nanomaterial for the Preparation of Intrinsically Flame-Retardant Materials. *Biomacromolecules* **2015**, *16*, 3399–3410. [CrossRef]
11. Hou, G.; Zhao, S.; Li, Y.; Fang, Z.; Isogai, A. Mechanically robust, flame-retardant phosphorylated cellulose films with tunable optical properties for light management in LEDs. *Carbohydr. Polym.* **2022**, *298*, 120129. [CrossRef] [PubMed]
12. Qing, Y.; Sabo, R.; Zhu, J.Y.; Agarwal, U.; Cai, Z.; Wu, Y. A comparative study of cellulose nanofibrils disintegrated via multiple processing approaches. *Carbohydr. Polym.* **2013**, *97*, 226–234. [CrossRef]
13. Rol, F.; Belgacem, N.M.; Gandini, A.; Bras, J. Recent advances in surface-modified cellulose nanofibrils. *Progr. Polymer. Sci.* **2019**, *88*, 241–264. [CrossRef]
14. Zhang, S.; Li, S.N.; Wu, Q.; Li, Q.; Huang, J.; Li, W.; Zhang, W.; Wang, S. Phosphorus containing group and lignin toward intrinsically flame retardant cellulose nanofibril-based film with enhanced mechanical properties. *Compos. B Eng.* **2021**, *212*, 108699. [CrossRef]
15. Saito, T.; Hirota, M.; Tamura, N.; Kimura, S.; Fukuzumi, H.; Heux, L.; Isogai, A. Individualization of nano-sized plant cellulose fibrils by direct surface carboxylation using TEMPO catalyst under neutral conditions. *Biomacromolecules* **2009**, *10*, 1992–1996. [CrossRef] [PubMed]
16. Wågberg, L.; Decher, G.; Norgren, M.; Lindström, T.; Ankerfors, M.; Axnäs, K. The build-up of polyelectrolyte multilayers of microfibrillated cellulose and cationic polyelectrolytes. *Langmuir* **2008**, *24*, 784–795. [CrossRef] [PubMed]
17. Henriksson, M.; Berglund, L.A.; Isaksson, P.; Lindström, T.; Nishino, T. Cellulose nanopaper structures of high toughness. *Biomacromolecules* **2008**, *9*, 1579–1585. [CrossRef]
18. Noguchi, Y.; Homma, I.; Matsubara, Y. Complete nanofibrillation of cellulose prepared by phosphorylation. *Cellulose* **2017**, *24*, 1295–1305. [CrossRef]
19. Rol, F.; Belgacem, N.; Meyer, V.; Petit-Conil, M.; Bras, J. Production of fire-retardant phosphorylated cellulose fibrils by twin-screw extrusion with low energy consumption. *Cellulose* **2019**, *26*, 5635–5651. [CrossRef]
20. Šturcová, A.; Davies, G.R.; Eichhorn, S.J. Elastic modulus and stress-transfer properties of tunicate cellulose whiskers. *Biomacromolecules* **2005**, *6*, 1055–1061. [CrossRef]
21. Lazar, S.T.; Kolibaba, T.J.; Grunlan, J.C. Flame-retardant surface treatments. *Nat. Rev. Mater.* **2020**, *5*, 259–275. [CrossRef]
22. Donius, A.E.; Liu, A.; Berglund, L.A.; Wegst, U.G.K. Superior mechanical performance of highly porous, anisotropic nanocellulose-montmorillonite aerogels prepared by freeze casting. *J. Mech. Behav. Biomed. Mater.* **2014**, *37*, 88–99. [CrossRef] [PubMed]
23. *EU Regulation 1907/2006: Candidate List of Substances of Very High Concern for Authorisation*; European Chemical Agency ECHA: Helsinki, Finland, 2006.
24. Laoutid, F.; Bonnaud, L.; Alexandre, M.; Lopez-Cuesta, J.M.; Dubois, P. New prospects in flame retardant polymer materials: From fundamentals to nanocomposites. *Mater. Sci. Eng. R Rep.* **2009**, *63*, 100–125. [CrossRef]
25. Available online: www.flameretardants-online.com/flame-retardants/market (accessed on 2 September 2023).
26. Hull, T.R.; Witkowski, A.; Hollingbery, L. Fire retardant action of mineral fillers. *Polym. Degrad. Stab.* **2011**, *96*, 1462–1469. [CrossRef]
27. Scharte, B. Phosphorus-based flame retardancy mechanisms-old hat or a starting point for future development? *Materials* **2010**, *3*, 4710–4745. [CrossRef] [PubMed]

28. Özer, M.S.; Gaan, S. Recent developments in phosphorus based flame retardant coatings for textiles: Synthesis, applications and performance. *Prog. Org. Coat.* **2022**, *171*, 107027. [CrossRef]

29. Weil, E.D. Fire-protective and flame-retardant coatings—A state-of-the-art review. *J. Fire Sci.* **2011**, *29*, 259–296. [CrossRef]

30. Schartel, B.; Braun, U.; Schwarz, U.; Reinemann, S. Fire retardancy of polypropylene/flax blends. *Polymer* **2003**, *44*, 6241–6250. [CrossRef]

31. Seefeldt, H.; Braun, U.; Wagner, M.H. Residue stabilization in the fire retardancy of wood-plastic composites: Combination of ammonium polyphosphate, expandable graphite, and red phosphorus. *Macromol. Chem. Phys.* **2012**, *213*, 2370–2377. [CrossRef]

32. Ishikawa, T.; Mizuno, K.; Kajiya, T.; Maki, I.; Koshizuka, T.; Takeda, K. Structural decay and flame retardancy of wood as a natural polymer. *Comb. Sci. Techn.* **2005**, *177*, 819–842. [CrossRef]

33. Kashiwagi, T.; Harris, R.H.; Zhang, X.; Briber, R.M.; Cipriano, B.H.; Raghavan, S.R.; Shields, J.R. Flame retardant mechanism of polyamide 6-clay nanocomposites. *Polymer* **2004**, *45*, 881–891. [CrossRef]

34. Gilman, J.W.; Jackson, C.L.; Morgan, A.B.; Harris, R.; Manias, E.; Giannelis, E.P.; Phillips, S.H. Flammability properties of polymer—Layered-silicate nanocomposites. Polypropylene and polystyrene nanocomposites. *Chem. Mater.* **2000**, *12*, 1866–1873. [CrossRef]

35. Fu, Q.; Medina, L.; Li, Y.; Carosio, F.; Hajian, A.; Berglund, L.A. Nanostructured wood hybrids for fire-retardancy prepared by clay impregnation into the cell wall. *ACS Appl. Mater. Interfaces* **2017**, *9*, 36154–36163. [CrossRef]

36. Chen, G.; Chen, C.; Pei, Y.; He, S.; Liu, Y.; Jiang, B.; Hu, L. A strong, flame-retardant, and thermally insulating wood laminate. *Chem. Eng. J.* **2020**, *383*, 123109. [CrossRef]

37. Guo, G.; Park, C.B.; Lee, Y.H.; Kim, Y.S.; Sain, M. Flame retarding effects of nanoclay on wood-fiber composites. *Polym. Eng. Sci.* **2007**, *47*, 330–336. [CrossRef]

38. Lee, Y.H.; Kuboki, T.; Park, C.B.; Sain, M.; Kontopoulou, M. The effects of clay dispersion on the mechanical, physical, and flame-retarding properties of wood fiber/polyethylene/clay nanocomposites. *J. Appl. Polym. Sci.* **2010**, *118*, 452–461. [CrossRef]

39. Kashiwagi, T.; Du, F.; Winey, K.I.; Groth, K.M.; Shields, J.R.; Bellayer, S.P.; Douglas, J.F. Flammability properties of polymer nanocomposites with single-walled carbon nanotubes: Effects of nanotube dispersion and concentration. *Polymer* **2005**, *46*, 471–481. [CrossRef]

40. Cabello-Alvarado, C.; Reyes-Rodríguez, P.; Andrade-Guel, M.; Cadenas-Pliego, G.; Pérez-Alvarez, M.; Cruz-Delgado, V.J.; Ávila-Orta, C.A. Melt-mixed thermoplastic nanocomposite containing carbon nanotubes and titanium dioxide for flame retardancy applications. *Polymers* **2019**, *11*, 1204. [CrossRef]

41. Grexa, O.; Poutch, F.; Manikova, D.; Martvonova, H.; Bartekova, A. Intumescence in fire retardancy of lignocellulosic panels. *Polym. Degrad. Stab.* **2003**, *82*, 373–377. [CrossRef]

42. Gavgani, J.N.; Adelnia, H.; Gudarzi, M.M. Intumescent flame retardant polyurethane/reduced graphene oxide composites with improved mechanical, thermal, and barrier properties. *J. Mater. Sci.* **2014**, *49*, 243–254. [CrossRef]

43. Esmailpour, A.; Majidi, R.; Taghiyari, H.R.; Ganjkhani, M.; Armaki, S.M.M.; Papadopoulos, A.N. Improving fire retardancy of beechwood by graphene. *Polymers* **2020**, *12*, 303. [CrossRef]

44. Bajwa, D.S.; Rehovsky, C.; Shojaeiarani, J.; Stark, N.; Bajwa, S.; Dietenberger, M.A. Functionalized cellulose nanocrystals: A potential fire retardant for polymer composites. *Polymers* **2019**, *11*, 1361. [CrossRef] [PubMed]

45. Bueno, A.B.F.; Bañón, M.V.N.; De Morentín, L.M.; García, J.M. Treatment of natural wood veneers with nano-oxides to improve their fire behaviour. In *IOP Conference Series: Materials Science and Engineering*; IOP Publishing: Philadelphia, PA, USA, 2014; Volume 64, pp. 1–6.

46. Ren, D.; Li, J.; Xu, J.; Wu, Z.; Bao, Y.; Li, N.; Chen, Y. Efficient antifungal and flame-retardant properties of ZnO-TiO$_2$-layered double-nanostructures coated on bamboo substrate. *Coatings* **2018**, *8*, 341. [CrossRef]

47. Deraman, A.F.; Chandren, S. Fire-retardancy of wood coated by titania nanoparticles. In *AIP Conference Proceedings*; American Institute of Physics Inc.: College Park, MD, USA, 2019; Volume 2155, p. 020022. [CrossRef]

48. Kashiwagi, T.; Gilman, J.W.; Butler, K.M.; Harris, R.H.; Shields, J.R.; Asano, A. Flame retardant mechanism of silica gel/silica. *Fire Mater.* **2000**, *24*, 277–289. [CrossRef]

49. Yang, L.; Mukhopadhyay, A.; Jiao, Y.; Yong, Q.; Chen, L.; Xing, Y.; Hamel, J.; Zhu, H. Ultralight, highly thermally insulating and fire resistant aerogel by encapsulating cellulose nanofibers with two-dimensional MoS$_2$. *Nanoscale* **2017**, *9*, 11452–11462. [CrossRef]

50. Mao, M.; Yu, K.X.; Cao, C.F.; Gong, L.X.; Zhang, G.D.; Zhao, L.; Song, P.; Gao, J.F.; Tang, L.C. Facile and green fabrication of flame-retardant Ti$_3$C$_2$T$_x$ MXene networks for ultrafast, reusable and weather-resistant fire warning. *Chem. Eng. J.* **2022**, *427*, 131615. [CrossRef]

51. Yu, B.; Tawiah, B.; Wang, L.Q.; Yuen, A.C.Y.; Zhang, Z.C.; Shen, L.L.; Yeoh, G.H. Interface decoration of exfoliated MXene ultra-thin nanosheets for fire and smoke suppressions of thermoplastic polyurethane elastomer. *J. Hazard. Mater.* **2019**, *374*, 110–119. [CrossRef]

52. Gogotsi, Y.; Anasori, B. The rise of MXenes. *ACS Nano* **2019**, *13*, 8491–8494. [CrossRef]

53. Nabipour, H.; Wang, X.; Song, L.; Hu, Y. Metal-organic frameworks for flame retardant polymers application: A critical review. *Compos. Part A Appl. Sci. Manuf.* **2020**, *139*, 106113. [CrossRef]

54. Nabipour, H.; Nie, S.; Wang, X.; Song, L.; Hu, Y. Highly flame retardant zeolitic imidazole framework-8@cellulose composite aerogels as absorption materials for organic pollutants. *Cellulose* **2020**, *27*, 2237–2251. [CrossRef]

55. Zhou, S.; Strømme, M.; Xu, C. Highly transparent, flexible, and mechanically strong nanopapers of cellulose nanofibers @metal–organic frameworks. *Chem.—A Eur. J.* **2019**, *25*, 3515–3520. [CrossRef]
56. Pan, Y.T.Z.; Zhang, Z.; Yang, R. The rise of MOFs and their derivatives for flame retardant polymeric materials: A critical review. *Compos. B Eng.* **2020**, *199*, 108265. [CrossRef]
57. Alongi, J.; Carletto, R.A.; Di Blasio, A.; Cuttica, F.; Carosio, F.; Bosco, F.; Malucelli, G. Intrinsic intumescent-like flame retardant properties of DNA-treated cotton fabrics. *Carbohydr. Polym.* **2013**, *96*, 296–304. [CrossRef] [PubMed]
58. Bosco, F.; Carletto, R.A.; Alongi, J.; Marmo, L.; Di Blasio, A.; Malucelli, G. Thermal stability and flame resistance of cotton fabrics treated with whey proteins. *Carbohydr. Polym.* **2013**, *94*, 372–377. [CrossRef]
59. Wang, X.; Hu, Y.; Song, L.; Xuan, S.; Xing, W.; Bai, Z.; Lu, H. Flame retardancy and thermal degradation of intumescent flame retardant poly(lactic acid)/starch biocomposites. *Ind. Eng. Chem. Res.* **2011**, *50*, 713–720. [CrossRef]
60. Costes, L.; Laoutid, F.; Brohez, S.; Dubois, P. Bio-based flame retardants: When nature meets fire protection. *Mater. Sci. Eng. R Rep.* **2017**, *117*, 1–25. [CrossRef]
61. Malucelli, G. Flame-retardant systems based on chitosan and its derivatives: State of the art and perspectives. *Molecules* **2020**, *25*, 4046. [CrossRef]
62. Réti, C.; Casetta, M.; Duquesne, S.; Bourbigot, S.; Delobel, R. Flammability properties of intumescent PLA starch and lignin. *Polym. Adv. Technol.* **2008**, *19*, 628–635. [CrossRef]
63. Sykam, K.; Försth, M.; Sas, G.; Restás, Á.; Das, O. Phytic acid: A bio-based flame retardant for cotton and wool fabrics. *Ind. Crops Prod.* **2021**, *164*, 113349. [CrossRef]
64. Kang, K.Y.; Kim, D.Y. Influence of sulfuric acid impregnation on the carbonization of cellulose. *J. Korean Phys. Soc.* **2012**, *60*, 1818–1822. [CrossRef]
65. Mishra, P.; Pavelek, O.; Rasticova, M.; Mishra, H.; Ekielski, A. Nanocellulose-Based Biomedical Scaffolds in Future Bioeconomy: A Techno-Legal Assessment of the State-of-the-Art. *Front. Bioeng. Biotechn.* **2022**, *9*, 789603. [CrossRef] [PubMed]
66. Lecoeur, E.; Vroman, I.; Bourbigot, S.; Lam, T.M.; Delobel, R. Flame retardant formulations for cotton. *Polym. Degrad. Stab.* **2001**, *74*, 487–492. [CrossRef]
67. Ghanadpour, M.; Carosio, F.; Ruda, M.C.; Wågberg, L. Tuning the Nanoscale Properties of Phosphorylated Cellulose Nanofibril-Based Thin Films to Achieve Highly Fire-Protecting Coatings for Flammable Solid Materials. *ACS Appl. Mater. Interfaces* **2018**, *10*, 32543–32555. [CrossRef]
68. Inagaki, N.; Nakamura, S.; Asai, H.; Katsuura, K. Phosphorylation of Cellulose with Phosphorous Acid and Thermal Degradation of the Product. *J. Appl. Polym. Sci.* **1976**, *20*, 2829–2836. [CrossRef]
69. Suflet, D.M.; Chitanu, G.C.; Popa, V.I. Phosphorylation of polysaccharides: New results on synthesis and characterisation of phosphorylated cellulose. *React. Funct. Polym.* **2006**, *66*, 1240–1249. [CrossRef]
70. Ablouh, E.H.; Brouillette, F.; Taourirte, M.; Sehaqui, H.; El Achaby, M.; Belfkira, A. A highly efficient chemical approach to producing green phosphorylated cellulosic macromolecules. *RSC Adv.* **2021**, *11*, 24206–24216. [CrossRef] [PubMed]
71. Kokol, V.; Božič, M.; Vogrinčič, R.; Mathew, A.P. Characterisation and properties of homo- and heterogenously phosphorylated nanocellulose. *Carbohydr. Polym.* **2015**, *125*, 301–313. [CrossRef]
72. Rol, F.; Sillard, C.; Bardet, M.; Yarava, J.R.; Emsley, L.; Gablin, C.; Bras, J. Cellulose phosphorylation comparison and analysis of phosphorate position on cellulose fibers. *Carbohydr. Polym.* **2020**, *229*, 115294. [CrossRef]
73. Fiss, B.G.; Hatherly, L.; Stein, R.S.; Friščić, T.; Moores, A. Mechanochemical Phosphorylation of Polymers and Synthesis of Flame-Retardant Cellulose Nanocrystals. *ACS Sustain. Chem. Eng.* **2019**, *7*, 7951–7959. [CrossRef]
74. Shi, Y.; Belosinschi, D.; Brouillette, F.; Belfkira, A.; Chabot, B. Phosphorylation of Kraft fibers with phosphate esters. *Carbohydr. Polym.* **2014**, *106*, 121–127. [CrossRef]
75. Wu, M.; Huang, Y.; Zhang, T.; Kuga, S.; Ewulonu, C.M. Cellulose nanofibril-based flame retardant and its application to paper. *ACS Sustain. Chem. Eng.* **2020**, *8*, 10222–10229.
76. Antoun, K.; Ayadi, M.; El Hage, R.; Nakhl, M.; Sonnier, R.; Gardiennet, C.; Brosse, N. Renewable phosphorous-based flame retardant for lignocellulosic fibers. *Ind. Crops Prod.* **2022**, *186*, 115265. [CrossRef]
77. Yuan, H.B.; Tang, R.C.; Yu, C.B. Flame retardant functionalization of microcrystalline cellulose by phosphorylation reaction with phytic acid. *Int. J. Mol. Sci.* **2021**, *22*, 9631. [CrossRef] [PubMed]
78. Božič, M.; Liu, P.; Mathew, A.P.; Kokol, V. Enzymatic phosphorylation of cellulose nanofibers to new highly-ions adsorbing, flame-retardant and hydroxyapatite-growth induced natural nanoparticles. *Cellulose* **2014**, *21*, 2713–2726. [CrossRef]
79. Gospodinova, N.; Grelard, A.; Jeannin, M.; Chitanu, G.C.; Carpov, A.; Thiéry, V.; Besson, T. Efficient solvent-free microwave phosphorylation of microcrystalline cellulose. *Green Chem.* **2002**, *4*, 220–222. [CrossRef]
80. Khakalo, A.; Jaiswal, A.K.; Kumar, V.; Gestranius, M.; Kangas, H.; Tammelin, T. Production of High-Solid-Content Fire-Retardant Phosphorylated Cellulose Microfibrils. *ACS Sustain. Chem. Eng.* **2021**, *9*, 12365–12375. [CrossRef]
81. Ghanadpour, M.; Carosio, F.; Wågberg, L. Ultrastrong and flame-resistant freestanding films from nanocelluloses, self-assembled using a layer-by-layer approach. *Appl. Mater. Today* **2017**, *9*, 229–239. [CrossRef]
82. Rol, F.; Karakashov, B.; Nechyporchuk, O.; Terrien, M.; Meyer, V.; Dufresne, A.; Belgacem, M. Pilot-Scale Twin Screw Extrusion and Chemical Pretreatment as an Energy-Efficient Method for the Production of Nanofibrillated Cellulose at High Solid Content. *ACS Sustain. Chem. Eng.* **2017**, *5*, 6524–6531. [CrossRef]

83. Gold, C. *Standard UL-94: Test for Flammability of Plastic Materials for Parts in Devices and Appliances*; Tech Notes: Washington, DC, USA, 2006; Volume II.

84. Velencoso, M.M.; Battig, A.; Markwart, J.C.; Schartel, B.; Wurm, F.R. Molekulare Brandbekämpfung—Wie moderne Phosphor-chemie zur Lösung der Flammschutzaufgabe beitragen kann. *Angew. Chem.* **2018**, *130*, 10608–106026. [CrossRef]

85. Carosio, F.; Kochumalayil, J.; Cuttica, F.; Camino, G.; Berglund, L. Oriented Clay Nanopaper from Biobased Components—Mechanisms for Superior Fire Protection Properties. *ACS Appl. Mater. Interfaces* **2015**, *7*, 5847–5856. [CrossRef]

86. Kiliaris, P.; Papaspyrides, C.D. Polymer/layered silicate (clay) nanocomposites: An overview of flame retardancy. *Progress. Polym. Sci.* **2010**, *35*, 902–958. [CrossRef]

87. Liu, A.; Walther, A.; Ikkala, O.; Belova, L.; Berglund, L.A. Clay nanopaper with tough cellulose nanofiber matrix for fire retardancy and gas barrier functions. *Biomacromolecules* **2011**, *12*, 633–641. [CrossRef] [PubMed]

88. Carosio, F.; Cuttica, F.; Medina, L.; Berglund, L.A. Clay nanopaper as multifunctional brick and mortar fire protection coating-Wood case study. *Mater. Des.* **2016**, *93*, 357–363. [CrossRef]

89. Carosio, F.; Kochumalayil, J.; Fina, A.; Berglund, L.A. Extreme thermal shielding effects in nanopaper based on multilayers of aligned clay nanoplatelets in cellulose nanofiber matrix. *Adv. Mater. Interfaces* **2016**, *3*, 1600551. [CrossRef]

90. Ming, S.; Chen, G.; He, J.; Kuang, Y.; Liu, Y.; Tao, R.; Fang, Z. Highly transparent and self-extinguishing nanofibrillated cellulose-monolayer clay nanoplatelet hybrid films. *Langmuir* **2017**, *33*, 8455–8462. [CrossRef] [PubMed]

91. Qin, S.; Pour, M.G.; Lazar, S.; Köklükaya, O.; Gerringer, J.; Song, Y.; Grunlan, J.C. Super gas barrier and fire resistance of nanoplatelet/nanofibril multilayer thin films. *Adv. Mater. Interfaces* **2019**, *6*, 1801424. [CrossRef]

92. Santos, L.P.; Da Silva, D.S.; Morari, T.H.; Galembeck, F. Environmentally friendly, high-performance fire retardant made from cellulose and graphite. *Polymers* **2021**, *13*, 2400. [CrossRef] [PubMed]

93. *ISO 1182:2020*; Reaction to Fire Tests for Products—Non-Combustibility Test. ISO: Geneva, Switzerland, 2020.

94. Miao, Y.; Wang, X.; Liu, Y.; Liu, Z.; Chen, W. Preparation of graphene oxide/cellulose composites with microcrystalline cellulose acid hydrolysis using the waste acids generated by the hummers method of graphene oxide synthesis. *Polymers* **2021**, *13*, 4453. [CrossRef]

95. Higginbotham, A.L.; Lomeda, J.R.; Morgan, A.B.; Tour, J.M. Graphite oxide flame-retardant polymer nanocomposites. *ACS Appl. Mater. Interfaces* **2009**, *1*, 2256–2261. [CrossRef]

96. Zhang, Z.; Yang, D.; Yang, H.; Li, Y.; Lu, S.; Cai, R.; Tan, W. A Hydrophobic Sisal Cellulose Microcrystal Film for Fire Alarm Sensors. *Nano Lett.* **2021**, *21*, 2104–2110. [CrossRef]

97. Cao, C.F.; Yu, B.; Guo, B.F.; Hu, W.J.; Sun, F.N.; Zhang, Z.H.; Wang, H. Bio-inspired, sustainable and mechanically robust graphene oxide-based hybrid networks for efficient fire protection and warning. *Chem. Eng. J.* **2022**, *439*, 134516. [CrossRef]

98. Qiu, S.; Ren, X.; Zhou, X.; Zhang, T.; Song, L.; Hu, Y. Nacre-Inspired Black Phosphorus/Nanofibrillar Cellulose Composite Film with Enhanced Mechanical Properties and Superior Fire Resistance. *ACS Appl. Mater. Interfaces* **2020**, *12*, 36639–36651. [CrossRef] [PubMed]

99. Xie, H.; Lai, X.; Li, H.; Gao, J.; Zeng, X.; Huang, X.; Lin, X. A highly efficient flame retardant nacre-inspired nanocoating with ultrasensitive fire-warning and self-healing capabilities. *Chem. Eng. J.* **2019**, *369*, 8–17. [CrossRef]

100. Zeng, Q.; Zhao, Y.; Lai, X.; Jiang, C.; Wang, B.; Li, H.; Chen, Z. Skin-inspired multifunctional MXene/cellulose nanocoating for smart and efficient fire protection. *Chem. Eng. J.* **2022**, *446*, 136899. [CrossRef]

101. Chollet, B.; Lopez-Cuesta, J.M.; Laoutid, F.; Ferry, L. Lignin nanoparticles as a promising way for enhancing lignin flame retardant effect in polylactide. *Materials* **2019**, *12*, 2132. [CrossRef] [PubMed]

102. Wu, Q.; Ran, F.; Dai, L.; Li, C.; Li, R.; Si, C. A functional lignin-based nanofiller for flame-retardant blend. *Int. J. Biol. Macromol.* **2021**, *190*, 390–395. [CrossRef]

103. Dai, P.; Liang, M.; Ma, X.; Luo, Y.; He, M.; Gu, X.; Luo, Z. Highly Efficient, Environmentally Friendly Lignin-Based Flame Retardant Used in Epoxy Resin. *ACS Omega* **2020**, *5*, 32084–32093. [CrossRef]

104. Zheng, C.; Li, D.; Ek, M. Improving fire retardancy of cellulosic thermal insulating materials by coating with bio-based fire retardants. *Nord. Pulp Paper Res. J.* **2019**, *34*, 96–106. [CrossRef]

105. Han, T.; Sophonrat, N.; Evangelopoulos, P.; Persson, H.; Yang, W.; Jönsson, P. Evolution of sulfur during fast pyrolysis of sulfonated Kraft lignin. *J. Anal. Appl. Pyrolysis* **2018**, *133*, 162–168. [CrossRef]

106. Tong, C.; Zhang, S.; Zhong, T.; Fang, Z.; Liu, H. Highly fibrillated and intrinsically flame-retardant nanofibrillated cellulose for transparent mineral filler-free fire-protective coatings. *Chem. Eng. J.* **2021**, *419*, 129440. [CrossRef]

107. Soares Bilhalva Dos Santos, P.; Fuentes Da Silva, S.; Labidi, J.; Gatto, D. Fire resistance of wood treated by emulsion from kraft lignin. *Drewno* **2016**, *59*, 199–204. [CrossRef]

108. Uddin, K.M.A.; Ago, M.; Rojas, O.J. Hybrid films of chitosan, cellulose nanofibrils and boric acid: Flame retardancy, optical and thermo-mechanical properties. *Carbohydr. Polym.* **2017**, *177*, 13–21. [CrossRef] [PubMed]

109. Pan, H.; Song, L.; Ma, L.; Pan, Y.; Liew, K.M.; Hu, Y. Layer-by-layer assembled thin films based on fully biobased polysaccharides: Chitosan and phosphorylated cellulose for flame-retardant cotton fabric. *Cellulose* **2014**, *21*, 2995–3006. [CrossRef]

110. Carosio, F.; Ghanadpour, M.; Alongi, J.; Wågberg, L. Layer-by-layer-assembled chitosan/phosphorylated cellulose nanofibrils as a bio-based and flame protecting nano-exoskeleton on PU foams. *Carbohydr. Polym.* **2018**, *202*, 479–487. [CrossRef]

111. Köklükaya, O.; Carosio, F.; Wågberg, L. Superior Flame-Resistant Cellulose Nanofibril Aerogels Modified with Hybrid Layer-by-Layer Coatings. *ACS Appl. Mater. Interfaces* **2017**, *9*, 29082–29092. [CrossRef]

112. Dorez, G.; Ferry, L.; Sonnier, R.; Taguet, A.; Lopez-Cuesta, J.M. Effect of cellulose, hemicellulose and lignin contents on pyrolysis and combustion of natural fibers. *J. Anal. Appl. Pyrolysis* **2014**, *107*, 323–331. [CrossRef]

113. Gao, C.; Zhou, L.; Yao, S.; Qin, C.; Fatehi, P. Phosphorylated kraft lignin with improved thermal stability. *Int. J. Biol. Macromol.* **2020**, *162*, 1642–1652. [CrossRef]

114. Zhang, T.; Yan, H.; Shen, L.; Fang, Z.; Zhang, X.; Wang, J.; Zhang, B. Chitosan/phytic acid polyelectrolyte complex: A green and renewable intumescent flame retardant system for ethylene-vinyl acetate copolymer. *Ind. Eng. Chem. Res.* **2014**, *53*, 19199–191207. [CrossRef]

115. Moussout, H.; Ahlafi, H.; Aazza, M.; Bourakhouadar, M. Kinetics and mechanism of the thermal degradation of biopolymers chitin and chitosan using thermogravimetric analysis. *Polym. Degrad. Stab.* **2016**, *130*, 1–9. [CrossRef]

116. Cogollo-Herrera, K.; Bonfante-Álvarez, H.; De Ávila-Montiel, G.; Barros, A.H.; González-Delgado, Á.D. Techno-economic sensitivity analysis of large scale chitosan production process from shrimp shell wastes. *Chem. Eng. Trans.* **2018**, *70*, 2179–2184.

117. Niu, F.; Wu, N.; Yu, J.; Ma, X. Gelation, flame retardancy, and physical properties of phosphorylated microcrystalline cellulose aerogels. *Carbohydr. Polym.* **2020**, *242*, 116422. [CrossRef] [PubMed]

118. Zhu, Y.; Yu, Z.; Zhu, J.; Zhang, Y.; Ren, X.; Jiang, F. Developing flame-retardant lignocellulosic nanofibrils through reactive deep eutectic solvent treatment for thermal insulation. *Chem. Eng. J.* **2022**, *445*, 136748. [CrossRef]

119. Carosio, F.; Medina, L.; Kochumalayil, J.; Berglund, L.A. Green and fire resistant nanocellulose/hemicellulose/clay foams. *Adv. Mater. Interfaces* **2021**, *8*, 2101111. [CrossRef]

120. Wang, L.; Sánchez-Soto, M. Green bio-based aerogels prepared from recycled cellulose fiber suspensions. *RSC Adv.* **2015**, *5*, 31384–31391. [CrossRef]

121. Han, Y.; Zhang, X.; Wu, X.; Lu, C. Flame Retardant, Heat Insulating Cellulose Aerogels from Waste Cotton Fabrics by in Situ Formation of Magnesium Hydroxide Nanoparticles in Cellulose Gel Nanostructures. *ACS Sustain. Chem. Eng.* **2015**, *3*, 1853–1859. [CrossRef]

122. He, C.; Huang, J.; Li, S.; Meng, K.; Zhang, L.; Chen, Z.; Lai, Y. Mechanically Resistant and Sustainable Cellulose-Based Composite Aerogels with Excellent Flame Retardant, Sound-Absorption, and Superantiwetting Ability for Advanced Engineering Materials. *ACS Sustain. Chem. Eng.* **2018**, *6*, 927–936. [CrossRef]

123. Fan, B.; Chen, S.; Yao, Q.; Sun, Q.; Jin, C. Fabrication of cellulose nanofiber/AlOOH aerogel for flame retardant and thermal insulation. *Materials* **2017**, *10*, 311. [CrossRef]

124. Yuan, B.; Zhang, J.; Yu, J.; Song, R.; Mi, Q.; He, J.; Zhang, J. Transparent and flame retardant cellulose/aluminum hydroxide nanocomposite aerogels. *Sci. China Chem.* **2016**, *59*, 1335–1341. [CrossRef]

125. Yuan, B.; Zhang, J.; Mi, Q.; Yu, J.; Song, R.; Zhang, J. Transparent cellulose-silica composite aerogels with excellent flame retardancy via an in situ sol-gel process. *ACS Sustain. Chem. Eng.* **2017**, *5*, 11117–11123. [CrossRef]

126. Farooq, M.; Sipponen, M.H.; Seppälä, A.; Österberg, M. Eco-friendly Flame-Retardant Cellulose Nanofibril Aerogels by Incorporating Sodium Bicarbonate. *ACS Appl. Mater. Interfaces* **2018**, *10*, 27407–27415. [CrossRef]

127. Guo, W.; Wang, X.; Zhang, P.; Liu, J.; Song, L.; Hu, Y. Nano-fibrillated cellulose-hydroxyapatite based composite foams with excellent fire resistance. *Carbohydr. Polym.* **2018**, *195*, 71–78. [CrossRef]

128. Yang, W.; Ping, P.; Wang, L.L.; Chen, T.B.Y.; Yuen, A.C.Y.; Zhu, S.E.; Wang, P.P.; Sun, C.; Zhang, C.Y.; Lu, H.D.; et al. Fabrication of Fully Bio-Based Aerogels via Microcrystalline Cellulose and Hydroxyapatite Nanorods with Highly Effective Flame-Retardant Properties. *ACS Appl. Nano Mater.* **2018**, *1*, 1921–1931. [CrossRef]

129. Huang, C.; Bhagia, S.; Hao, N.; Meng, X.; Liang, L.; Yong, Q.; Ragauskas, A.J. Biomimetic composite scaffold from an in situ hydroxyapatite coating on cellulose nanocrystals. *RSC Adv.* **2019**, *9*, 5786–5793. [CrossRef] [PubMed]

130. Ghanadpour, M.; Wicklein, B.; Carosio, F.; Wågberg, L. All-natural and highly flame-resistant freeze-cast foams based on phosphorylated cellulose nanofibrils. *Nanoscale* **2018**, *10*, 4085–4095. [CrossRef]

131. Wicklein, B.; Kocjan, A.; Salazar-Alvarez, G.; Carosio, F.; Camino, G.; Antonietti, M.; Bergström, L. Thermally insulating and fire-retardant lightweight anisotropic foams based on nanocellulose and graphene oxide. *Nat. Nanotechnol.* **2015**, *10*, 277–283. [CrossRef] [PubMed]

132. Wicklein, B.; Kocjan, D.; Carosio, F.; Camino, G.; Bergström, L. Tuning the nanocellulose-borate interaction to achieve highly flame retardant hybrid materials. *Chem. Mater.* **2016**, *28*, 1985–1989. [CrossRef]

133. Cheng, X.; Zhu, S.; Pan, Y.; Deng, Y.; Shi, L.; Gong, L. Fire retardancy and thermal behaviors of Cellulose nanofiber/zinc borate aerogel. *Cellulose* **2020**, *27*, 7463–7474. [CrossRef]

134. Guo, W.; Hu, Y.; Wang, X.; Zhang, P.; Song, L.; Xing, W. Exceptional flame-retardant cellulosic foams modified with phosphorus-hybridized graphene nanosheets. *Cellulose* **2019**, *26*, 1247–1260. [CrossRef]

135. Assi, H.; Mouchaham, H.; Steunou, N.; Devic, T.; Serre, C. Titanium coordination compounds: From discrete metal complexes to metal-organic frameworks. *Chem. Soc. Rev.* **2017**, *46*, 3431–3452. [CrossRef]

136. Zhou, S.; Apostolopoulou-Kalkavoura, V.; Tavares da Costa, M.V.; Bergström, L.; Strømme, M.; Xu, C. Elastic Aerogels of Cellulose Nanofibers@Metal–Organic Frameworks for Thermal Insulation and Fire Retardancy. *Nanomicro. Lett.* **2020**, *12*, 1–13. [CrossRef]

137. Zhang, J.; Ji, Q.; Shen, X.; Xia, Y.; Tan, L.; Kong, Q. Pyrolysis products and thermal degradation mechanism of intrinsically flame-retardant calcium alginate fibre. *Polym. Degrad. Stab.* **2011**, *96*, 936–942. [CrossRef]

138. Berglund, L.; Nissilä, T.; Sivaraman, D.; Komulainen, S.; Telkki, V.V.; Oksman, K. Seaweed-derived alginate-cellulose nanofiber aerogel for insulation applications. *ACS Appl. Mater. Interfaces* **2021**, *13*, 34899–34909. [CrossRef] [PubMed]

139. Missio, A.L.; Otoni, C.G.; Zhao, B.; Beaumont, M.; Khakalo, A.; Kämäräinen, T.; Rojas, O.J. Nanocellulose Removes the Need for Chemical Crosslinking in Tannin-Based Rigid Foams and Enhances Their Strength and Fire Retardancy. *ACS Sustain. Chem. Eng.* **2022**, *10*, 10303–10310. [CrossRef] [PubMed]
140. Lavoine, N.; Bergström, L. Nanocellulose-based foams and aerogels: Processing, properties, and applications. *J. Mater. Chem. A* **2017**, *5*, 16105–16117. [CrossRef]
141. Apostolopoulou-Kalkavoura, V.; Munier, P.; Bergström, L. Thermally Insulating Nanocellulose-Based Materials. *Adv. Mater.* **2021**, *33*, 2001839–2001856. [CrossRef]
142. Isogai, A. Emerging Nanocellulose Technologies: Recent Developments. *Adv. Mater.* **2020**, *33*, 1–10. [CrossRef]